Mathematical Modelling and Optimization Analysis of Malaria infection in the presence of Insecticide Resistance and Climate Variations in Kenya

Lorna Chepkemoi

167083

Submitted in Partial Fulfillment of the Requirements for the Degree of Master of Science in Biomathematics at Strathmore University

Strathmore Institute of Mathematical Sciences
Strathmore University
Nairobi, Kenya

June, 2025

Declaration and Approval

Declaration

I declare that this work has not been previously submitted and approved for the award of a degree by this or any other University. To the best of my knowledge and belief, the thesis contains no material previously published or written by another person except where due reference is made in the research thesis itself.

Student's Name: **Lorna Chepkemoi**

Signature: _____

Date: May 22, 2025

Approval

The thesis of **Lorna Chepkemoi** was reviewed and approved for examination by the following:

Prof. Samuel Mwalili,
Supervisor, Strathmore Institute of Mathematical Sciences,
Strathmore University

Dr. Titus Orwa,
Supervisor, Strathmore Institute of Mathematical Sciences,
Strathmore University

Dr. Godfrey Madigu,
Dean, Strathmore Institute of Mathematical Sciences,
Strathmore University

Prof. Bernard Shibwabo,
Director, Office of Graduate Studies,
Strathmore University

Acknowledgements

I would like to first thank God for the good health and strength He has given me. Secondly, I would like acknowledge the contribution of my supervisors, Prof. Samuel Mwalili and Dr. Titus Orwa from the Institute of Mathematical Sciences, Strathmore University, as well as Dr. Henry Tonnang and Dr. Daisy Salifu from International Centre of Insect Physiology and Ecology. It is through their dedication and conscientious efforts that the conceptualization of this research has come to fruition.

Table of Contents

List of Figures

List of Tables

List of Abbreviations

ACT	Artemisinin based combination therapy
COVID-19	Coronavirus disease
FBSM	Forward-backward sweep method
GTS	Global Technical Strategy
IRS test	Insecticide residual spraying
kdr	Knock-down resistance
LLINs	Long lasting insecticide treated nets
vgsc	Voltage gated sodium channel
WHO	World Health Organization

Abstract

Over the years, control efforts to curb malaria transmission have been initiated and implemented by World Health Organization (WHO). These control efforts however rely on the use of insecticide based control interventions which has enhanced the emergence and persistence of insecticide resistance to almost every insecticide class used. This study determines the optimal combination strategies for malaria control in the presence of insecticide resistance and climatic variation in Kenya. A deterministic model representing malaria transmission dynamics in the human and mosquito population is formulated and studied. The model equations are solved numerically using fourth and fifth order Runge-Kutta methods while the optimal control framework is solved numerically using forward-backward sweep method. The basic reproduction number R_0 is derived and the disease free equilibrium is shown to be locally and globally asymptotically stable. Sensitivity analysis reveals that the resting rate of susceptible mosquitoes α_s and the mosquito mortality rate due to the use of insecticides δ_v are the most influential parameters in determining malaria transmission dynamics. Numerical simulation results show that in the presence of insecticide resistance, R_0 is 1.2721 implying that malaria disease persists in the population. The spatial distribution of the reproduction number across Kenya further show that regions whose climatic conditions are favourable for malaria vector survival experience higher malaria transmission compared to areas whose climatic conditions are less favourable for vector survival and development. Additionally, based on optimal control analysis, the best malaria control intervention is when personal protection, treatment and vaccination are used simultaneously. This study reveals that insecticide resistance and climatic variation have a significant impact in the spread of malaria. Therefore, the study's findings can be adopted by national malaria control program stakeholders in the fight against malaria in Kenya.

Chapter 1: Introduction

1.1 Background to the Study

Malaria is a life threatening disease found in most parts of the world including the tropical and subtropical regions, especially in Africa, Asia, Latin America, the Middle East and some parts of Europe (Tumwiine et al., 2007; Azu-Tungmah et al., 2019). Although malaria is both preventable and treatable, it is one of the leading causes of mortality globally with children and pregnant women being most vulnerable (Olutimo et al., 2024). According to the 2024 World Health Organization (WHO) report on malaria status, there were an estimated 263 million new malaria cases and 597,000 malaria deaths in the world with African region accounting for 95% of the total malaria cases (WHO, 2024). Among the malaria cases in Africa, Ethiopia, Nigeria and Uganda bore the greatest burden of increase in malaria cases of 1.3 million, 1.3 million and 597, 000, respectively (WHO, 2024).

The disease burden in Africa has been enhanced by low socio-economic and educational status especially in the rural and poor zones (Romero-Leiton and Ibargüen-Mondragón, 2019; Ngandu et al., 2020; Darteh et al., 2021), with the changing climatic conditions accelerating the survival and reproduction rate of malaria vectors (Mieguim Ngninpogni et al., 2021; Nkiruka et al., 2021). Additionally, other factors such as the prolonged effects of COVID-19 on service delivery, limited healthcare access, inadequate funding, drug and insecticide resistance, ongoing conflicts and emergencies and uneven implementation of core malaria interventions continue to enhance the persistence of malaria disease in sub-Saharan Africa.

In Kenya, about 6.7 million malaria cases are reported yearly, with 70% of the population being at risk of the disease and 13–15% of outpatient consultations being malaria cases (Sultana et al., 2017; Elnour et al., 2023). Climatic factors such as altitude, temperature, and rainfall patterns continue to influence malaria transmission and infection risk in Kenya with its prevalence varying across seasons and regions (USAID, 2017). In the lake and coastal regions, malaria transmission is high as the climatic conditions are suitable for the survival of malaria vector. In the highland regions, malaria transmission is seasonal with annual variation experienced in the area (USAID, 2017; Kenya, 2020). With favourable climatic conditions, the breeding of malaria vector is sustained, increasing the

transmission intensity of the disease (Kenya, 2020). Consequently, this will introduce malaria disease in regions where it did not exist before.

Control interventions to curb malaria transmission have been initiated and implemented by WHO over the years. In 2015, The Global Technical Strategy (GTS) was launched whose goals was to achieve a reduction of malaria mortality and case incidence by 40% in 2020, by 75% in 2025, and by 90% in 2030 (WHO, 2015). However, by 2017, there were no significant improvements towards these global goals and this prompted the launch of WHO "High burden to high impact" initiative, which made a call to mobilise resources for intensified efforts in the eleven highest-burden countries (WHO, 2018).

Inspite of the efforts made, the global malaria response has faced a growing number of threats and of key concern is insecticide resistance and climate change (WHO, 2023). Insecticide resistance has been of key concern as present malaria control measures have been limited to synthetic pyrethroids for long lasting insecticide treated nets (LLINs) and insecticide residual spraying (IRS) (Metchanun, 2020). Additionally, climatic variations have influenced mosquito development, their feeding frequency, survival and parasite development inside the mosquito enhancing malaria transmission (Patz et al., 2003; Sutherst, 2004). Emerging resistance to pyrethroids and climate change threaten the previous gains and render achieving malaria elimination in the near future elusive (WHO, 2023). There is therefore need to continually conduct research to enhance malaria control interventions and reduce malaria incidence and mortality rates.

Over decades, mathematical models have been one of the widely used tools to gain better knowledge and insights of malaria disease in terms of transmission dynamics and assessing the effectiveness of control interventions. The models have proven to be useful due to their increased predictive computational capability. Malaria models originated from the works of Ross and Macdonald (Mandal et al., 2011), and have continuously been refined by the scientific community to capture the dynamical changes in the transmission. Some of the changes being the development of resistance to the currently used insecticides reducing their effectiveness and the rising impacts of climate change on malaria transmission (WHO, 2024).

Factors affecting malaria transmission

Insecticide resistance

Insecticide resistance is the ability of a mosquito to tolerate the effects of an insecticide by becoming resistant to its toxic effects. Insecticide resistance mechanism can be categorized into four i.e., i) target site resistance induced by alteration of insecticide binding due to mutation in the specific binding site of an insecticide reducing its effect; ii) metabolic resistance which is the degradation of insecticide molecules by detoxifying enzymes such as Cytochrome P450 monooxygenases, Glutathione S-transferases, esterases and hydrolases; iii) cuticular resistance caused by cuticular thickening which slows insecticides penetration; iv) behavioural resistance attributed to changes in malaria vector activity such as avoiding surfaces treated with insecticides (Mitchell et al., 2012; Edi et al., 2014; Hancock et al., 2018). Of the four insecticide resistance mechanism, target site and metabolic resistances are most likely to lead to the failure of insecticide-based control interventions (Sheldon and Verhulst, 1996). For target site resistance, a change in the amino acid sequence of the voltage gated sodium channel (vgsc) leads to a mechanism known as knock-down (kdr) resistance associated with pyrethroids or organochlorines (Donnelly et al., 2009; Barnes et al., 2017), while a change in amino acid occurring at neurotransmitter acetyl-cholinesterase leads to a mechanism called ace-1 resistance associated with organophosphates and carbamates (Djogbénou et al., 2009). For metabolic resistance, detoxification enzymes are expressed eliminating xenobiotic compounds such as insecticides before reaching their target sites (malERA Consultative Group on Vector Control, 2011).

Climatic factors

Mosquito vectors are essential to the spread of malaria, and their distribution is based on the suitability, productivity, and availability of breeding habitats (Castro, 2017). The availability of breeding habitats is influenced by precipitation, topography and hydrology, whereas the abundance of plant and predator species determines their suitability. Temperature affects the breeding habitat's productivity, the frequency at which mosquitoes feed on blood, larval stage development and the speed of parasite development. Increase in temperature in the range 18-32℃, accelerates anopheles species egg laying frequency

and their development rate. It also reduces the time it takes for the parasites to develop into infectious sporozoites inside the mosquitoes. The average life span of a female *An. gambiae* is about 21 days. However, at 18℃, it takes the malaria parasite 56 days to mature inside the mosquito, which is longer than the average lifespan of the mosquito, 19 days at 22℃ and 8 days at 30℃ (Diouf et al., 2020; Agyekum et al., 2021; Tuno et al., 2023).

On the other hand, rainfall increases mosquito population by providing suitable larval habitat for breeding and can also influence it negatively. Relative humidity between 55% and 80% reduces mosquito lifespans to such an extent that it limits the potential for malaria transmission by inhibiting Plasmodium from fully developing (Bhattacharya et al., 2006). Additionally, excessive rainfall can flush larval breeding sites leading to a decline in malaria transmission. Floods can also hinder malaria control measures by destroying health infrastructures in the region or can lead to migration of people into malaria endemic regions. With the availability of suitable breeding places, mosquito populations rapidly grow shortly after the start of the rainy season. However, the population can drastically drop with a following dry season to levels that malaria transmission cannot be sustained (Yanda et al., 2006). This explains the seasonal variations in malaria transmission.

1.2 Statement of the Problem

In sub-Saharan Africa, resolute control efforts to combat malaria transmission has been implemented since 2017 leading to a decline of malaria incidence and mortality by 42% and 66%, respectively (Riveron Miranda et al., 2018; Mohammed-Awel and Gumel, 2023). Interventions such as early diagnosis, improved drug therapy and better public health infrastructure, have contributed to this decline with the use of long lasting insecticidal nets (LLINs) and indoor residual spraying (IRS) contributing greatly to such success (Riveron Miranda et al., 2018; Bisanzio et al., 2022). During the period 2000-2015, it was estimated that there was an 81% reduction in malaria burden due to the use of LLINs and IRS (Bhatt et al., 2015). Globally, there are now renewed efforts to eradicate malaria by 2030 or 2040, with these efforts relying on the use of insecticide based control interventions such as pyrethroids-based LLINs and IRS (Barbosa and Hastings, 2012; Huijben and Paaijmans, 2018; Mohammed-Awel et al., 2018). The widespread use

of these insecticide-based interventions has led to the emergence of vector insecticide resistance to almost every insecticide class used in LLINs and IRS (Riveron Miranda et al., 2018).

Additionally, climatic variation especially in temperature and rainfall patterns, has provided suitable conditions for the development, feeding, breeding and survival of mosquitoes (Mordecai et al., 2019). For instance, a study carried out in western Kenya showed that variability in temperature and rainfall strongly influenced malaria incidence in the region (Nyawanda et al., 2023). Furthermore, in the northern region of Kenya, changes in rainfall patterns has created more breeding sites for malaria vectors putting more areas at risk of malaria epidemics (Lacave, 2023). Although recommendations have been provided by WHO to address the issue of pyrethroid resistance by using a combination of pyrethroid and synergist in LLINs instead of pyrethroid-only LLINS (WHO guidelines, 2023), the issue of climate change is a combined effort as it is contributed by human related activities such as deforestation. There is therefore a need to educate the public on the dire impact of climate change and its contribution to malaria transmission. Of importance also is incorporating climatic factors in studying the dynamics of malaria transmission and determining the effectiveness of existing control interventions such as use of insecticides, antimalarial therapies and vaccination under such climatic variability. This dynamical change has been well captured by the use of mathematical models, which have proven to be cost effective in such analysis. From studies by Ngonghala et al. (2012), mosquito behaviour i.e breeding, feeding and resting behaviours have been shown to contribute to malaria transmission. This study therefore will extend the work of Montoya and Romero-Leiton (2020) by stratifying mosquito population based on the feeding and resting behaviours and incorporating climate dependent parameters in the model. The study seeks to determine the optimal combination of control strategies that can be adopted in Kenya in the presence of insecticide resistance and climatic variability.

1.3 Research Objectives

1.3.1 General Objective

To determine optimal combination strategies for malaria control in the presence of insecticide resistance and climatic variations in Kenya.

1.3.2 Specific Objectives

The specific objectives for this study are:

1. To develop and analyse a mathematical model of malaria transmission under insecticide resistance and climatic variations in Kenya.
2. To investigate the impact of insecticide use on malaria prevalence in the absence and presence of insecticide resistance.
3. To implement an optimal control framework for reducing malaria burden in different regions of Kenya.

1.4 Significance of the Study

The WHO Global technical strategy (GTS) for malaria 2016-2030 called for reductions in malaria case incidence and mortality rates of at least 75% by 2025 and 90% by 2030, compared to a 2015 baseline (WHO, 2021). However, with the multiple threats that continue to hinder the response efforts such as drug and insecticide resistance, climate change, limited access to healthcare, inadequate funding and ongoing conflicts and emergencies, attaining 2025 target of the WHO global malaria strategy may be unfeasible. To achieve malaria free future, concerted efforts to reduce the effects of the impending threats is necessary. With the rising trends in insecticide resistance and climate change, integrated approaches are needed to reduce the effects of climate change at the same time controlling malaria transmission. Climate variability has indirectly impacted malaria trends through the disruptions of supply chains of LLINs, antimalarial medicines and vaccines (WHO, 2023). Further, due to climate-induced factors such as flooding, population displacement for example in Kenya has been evident with individuals migrating to malaria endemic areas hence the upsurge in malaria transmission (Lacave, 2023). With limited knowledge of the effectiveness of the existing control interventions amidst the ranging threats, using

mathematical models that incorporate most of these factors is necessary. This will inform national malaria control programs stakeholders on case management of the disease and can be used to evaluate the effectiveness of existing control interventions in Kenya. With better control interventions of malaria disease, the WHO Global technical strategy will be attainable.

1.5 Scope of the Study

In this study, a mathematical model is formulated based on the concept of compartmental model. The human population is categorized into two compartments: susceptible and infected classes, while the mosquito population is stratified based on the behaviour, into susceptible resting, infected resting, susceptible questing and infected questing mosquitoes. Qualitative analysis such as well posedness of the model, existence and stability of equilibrium points is carried out. For the numerical analysis, the initial conditions and parameter values are extracted from literature and the mosquito mortality rate due to the use of insecticides estimated using Vector Atlas data. The parameter estimates are obtained using maximum likelihood estimation method.

Climate dependent parameters are incorporated in the expression of the reproduction number to determine the influence of temperature and rainfall in malaria transmission. Temperature and rainfall raster for Kenya with an approximately 1km spatial resolution are obtained from EnviDat database (Karger et al., 2019).

Chapter 2: Literature Review

2.1 Malaria Biology

Malaria is caused by parasites of the genus *Plasmodium*. *Plasmodium falciparium*, *P. vivax*, *P. ovale*, *P. malariae* and *P. knowlesi* are the only parasites out of over 120 species of genus *Plasmodium* that causes malaria (WHO, 2015). *P. falciparum* causes the greatest burden in sub-saharan Africa, as the local epidemiology permits transmission of this parasite (Gething et al., 2011; Johnston et al., 2013; Mohammed-Awel and Gumel, 2023). The *plasmodium* parasite is transmitted by female anopheles (*An.*) mosquitoes with *An. gambiae sensu stricto*, *An. arabiensis*, *An. colluzzi*, *An. funestus sensu lato* and the new emergent vector, *An. stephensis* being of particular importance in these regions (Faulde et al., 2014).

Malaria infection begins when a plasmodium infected female anopheles mosquito bites a human host. The infected mosquito injects sporozoites that migrate to the liver through the blood stream and infect the liver cells initiating asexual replication of the parasite (Long and Zavala, 2017). The parasites are released from the liver into the red blood cells in the form of merozoites where they continue to multiply until the cell bursts. The released merozoites infect other red blood cells leading to the formation of infected red blood cells (Dhangadamajhi et al., 2010). The repetitions of bursting infected red blood cells and invasions of vulnerable red blood cells by merozoites triggers symptoms such as headaches, chills, fevers and nausea (Dhangadamajhi et al., 2010; Su et al., 2020). Some merozoites sexually differentiate into male and female gametocytes, which are ingested by a mosquito as they take up a blood meal from an infected human host (Su et al., 2020) and the cycle is repeated again.

2.2 Mathematical Modelling of Malaria

According to groups such as Malaria Eradication Research Agenda (MalERA) consultative group on modelling, mathematical modelling has been recognized as one of the tools to eradicate malaria globally. Some of the key areas where modelling has provided valuable insights include, optimal resource allocation, case management of drug and insecticide resistance, evaluation of new tools and combination of tools aimed at preventing malaria transmission, coverage targets and anticipated timeframes for achieving

elimination goals and operational feasibility assessment (malERA Consultative Group on Vector Control, 2011).

Mathematical modelling of malaria began with the model developed by Ross in 1911, investigating the relationship between the number of mosquitoes and incidence of malaria in humans (Ross, 1911). Ross's model divided the human population into susceptible (S_h) and infected (I_h) compartments with the infected class returning to susceptible class leading to an SIS model. Mosquito population had the susceptible and infected compartments only. In 1950s, Macdonald (1956) modified Ross's model by incorporating latency period in mosquitoes due to malaria parasite development. Therefore, the mosquito population was divided into susceptible, exposed and infected (SEI) classes. Anderson and May (1991) later introduced latency period of the parasite in humans by modifying Macdonald's model. This divided the human population into susceptible, exposed, infected and susceptible (SEIS) classes along with the SEI model of mosquito population. Overtime, the scientific community have modified Ross and Macdonald models to include various disease dynamics such as disease biology, interventions, spatial distribution, effect of age structure on prevalence, migration of people, parasite diversity, human immunity and resistance (Bailey, 1982; Anderson and May, 1991; Koella, 1991; Dietz et al., 1974; Torres-Sorando and Rodrıguez, 1997).

Studies have been done using these models to study disease transmission and assess the effectiveness of control interventions in various disease dynamics. For instance, a study by Chitnis et al. (2008b) developed a linear difference equation model depicting female mosquitoes' survival and their infection status. They used their model to simulate the impact of increasing LLIN coverage revealing that LLINs were effective in reducing malaria transmission. Griffin et al. (2010) highlighted that if high and sustained LLINs usage levels are maintained, malaria transmission levels will be reduced to low levels in low malaria transmission setting. Additionally, the study findings of Pongtavornpinyo et al. (2008) revealed that at high coverage rates, use of artemisinin based combination therapy (ACT) slows the spread of drug resistance to a partner drug in low malaria transmission settings. Chiyaka et al. (2009) developed a mathematical model for malaria treatment and spread of drug resistance in an endemic population. Based on the ratio of treated to untreated infectious periods and the rates of transmission from infected persons with resistant and sensitive diseases, the study's findings indicated that treatment as a control

strategy could slow down the spread of drug resistance.

Overtime, optimal control strategies have been applied in various malaria disease models to determine the best combination of control interventions to reduce malaria transmission. For instance, Orwa et al. (2021) formulated an in-host *P. falciparum* malaria model to study optimal malaria control strategies within the human host. Numerical simulation revealed that a combination of pre-erythrocytic vaccine antigen, blood schizontocide and gametocytocide drugs offerred the best strategy to eradicate clinical *P. falciparum* malaria. Additionally, Tchoumi et al. (2021) formulated a multi-stage malaria model and investigated an optimal control strategy using insecticide bed nets as control parameter. The study's findings revealed that reduction in bed net efficacy is compensated by the benefit of the number of susceptible/infected individuals excluded from the malaria disease dynamics. Tchoumi et al. (2022) formulated a susceptible-vaccinated-exposed-infected-recovered-susceptible SVEI(R)S malaria model for the human population, and SEI for the mosquito population. Numerical simulations revealed that a combination of personal protection, treatment, and vaccination of children under-five proved to be the best optimal control strategy instead of a single or any dual combination of the interventions at a specific time. Cai et al. (2022) formulated an SEIR model for the human population, SEI for the wild mosquitoes and an additional class for the sterile mosquitoes. An optimal control problem was formulated to minimize the number of infected humans and the cost of implementing two control strategies: use of LLINs and the release of sterile mosquitoes. The results indicated that combination of the two control strategies reduced the number of wild mosquitoes, consequently suppressing malaria transmission.

In spite of the stringent control interventions implemented to curb vector borne diseases, insecticide resistance threats continue to hamper the gains made to control the diseases. For instance, a study by Coffield et al. (2023) highlighted vector insecticide resistance being a possible cause of failure of control interventions against Chagas disease in Gran Chaco, Argentina. Another study by Bisanzio et al. (2022) used a spatio-temporal model to study the geo-spatial distribution of Anopheles gambiae sensu lato insecticide resistance in Tanzania for the 2011-2017 period. The model's output indicated that resistance to pyrethroids, organophosphates, organochlorines and carbamates was expected to exist in 19.5%, 11.6%, 8.1% and 15.6% of Tanzania's territory, respectively. Additionally, Mohammed-Awel et al. (2018) developed a deterministic model to assess the impact of

mosquito insecticide resistance on transmission dynamics of malaria at the population level in Ethiopia. Mosquito population was stratified based on type (wild or resistant to insecticides) and feeding preference (indoor or outdoor). According to the model's simulations, use of LLINs alone or in combination with IRS was more effective than a single deployment of IRS only strategy. Furthermore, numerical simulations demonstrated that the combined optimal LLINs-IRS strategy could result in the effective control of the disease and insecticide resistance effectively managed during the first eight years of the 15-year implementation period of the insecticides-based anti-malaria control measures in Ethiopia.

Although insecticide resistance can lead to an increase in malaria transmission, there is evidence that insecticide resistance declines with age. Saddler and Koella (2015) formulated a mathematical model that predicted how the decline of resistance with the age of a mosquito affected malaria transmission intensity. The study's finding revealed that there was a decrease of between 1.37% to 9.71% per day in phenotypic resistance independent of mosquito strain or species. The results implied a reduction on the predicted influence of insecticide resistance on the effectiveness of malaria control strategies.

The impact of seasonality on vector borne disease transmission has also been investigated in various studies. Yang and Ferreira (2000) noted that an increase in temperature in a low transmission area produces a deteriorating social and economic conditions. Consequently, about 34.5% of the susceptible individuals in a population moves to the exposed group and they show the possibility of reproduction number, R_0 being greater than 1 in some areas in the world. They concluded by highlighting the importance of social and economic effects more than temperature effects and further emphasized that good malaria control interventions and a good healthcare system can overcome the negative effects of increased temperature. Li et al. (2002) developed a SEIR model for human population where a record of prior illness is kept. A submodel of the mosquito population with divisions for juveniles and adults was also included. They input their malaria transmission model with the steady state value of the adult mosquito population obtained from this submodel, then determine the reliance of the reproductive number, for the whole malaria model, on an environmental parameter (such as temperature or rainfall), and then incorporate the dependence of the parameters for the mosquito population submodel on this parameter. Additionally, Ngarakana-Gwasira et al. (2016) formulated a mathematical

model incorporating rainfall and temperature to study malaria transmission dynamics in Africa. The human population was subdivided into SEIR classes while the mosquito population was first divided into juvenile and adult population and the adult population further subdivided into SEI classes. With the use of geographic information system (GIS), the reproduction number is applied to gridded temperature and rainfall records for the baseline and future climates. The model's results suggested that temperature and rainfall ranges of 30-32℃ and 15-17mm, respectively, are the optimum temperature and ideal rainfall for malaria transmission by *plasmodium falciparum* in Africa. Furthermore, as suggested by the study's results, there will be an increasing problem of endemic malaria in the African highlands due to climate change.

Other studies have incorporated climate variability in existing models and assessed the effectiveness of malaria control interventions in such dynamics. For instance, Herdicho et al. (2021) developed an S-I model for mosquito population, susceptible (S_h), exposed human with short-term incubation period subpopulation (E_{sh}), exposed human with long-term incubation period subpopulation (E_{lh}), infectious human subpopulation (I_h), and recovered human subpopulation (R_h) model. A seasonal factor was incorporated in the model and optimal control variables applied in the form of insecticide, prevention, and treatment. The model's numerical simulation showed that simultaneously providing controls in the form of insecticide, prevention, and treatment reduced the exposed and infectious human population and infectious mosquito population. Further, Keno et al. (2022) developed an SEIRS and SEI models for human population and mosquito population, respectively. They incorporated the impact of climate variability (temperature and rainfall) with respect to mosquitoes breeding rate and malaria infection in their model. Additionally, optimal control and cost effectiveness analysis were also performed. The model's numerical simulation revealed that use of insecticide treated nets and treatment were the optimal combination and cost effective strategies to minimize malaria transmission.

The abundance of models discussed is a result of the necessity to understand various aspects of the intricate malaria epidemiology. In the model to be analyzed, we aim to extended the existing models and stratify mosquito population based on mosquito behaviour that is questing and resting behaviour. Additionally, since insecticide resistance is a threat that has been highlighted as contributing to malaria transmission, the

model analysis is done in the presence of insecticide resistance. Climatic variability is incorporated by using parameters that are dependent on environmental factors such as temperature and rainfall. The context of the study is Kenya, therefore environmental variables for Kenya are used. Using numerical simulations, the most efficient combination of interventions, considering insecticide resistance and climatic factors, for reducing malaria burden in different regions of Kenya is obtained.

Chapter 3: Research Methodology

3.1 Introduction

This chapter presents the model formulation and the corresponding mathematical analysis. The model was solved numerically using fourth and fifth order Runge-Kutta method implemented via the `solve_ivp` function in Python. Additionally, the optimal control framework is developed by applying the Pontryagin's Maximum Principle and solved numerically using forward-backward sweep method. Details of the numerical methods are provided in Appendix E.

3.2 Model Formulation and Description

A mathematical model for malaria transmission in the presence of insecticide resistance is formulated. The compartmental model is composed of human and mosquito populations. The total human population, $N_h(t)$ consists of the susceptible $S_h(t)$ and infected $I_h(t)$ humans. Hence,

$$N_h(t) = S_h(t) + I_h(t).$$

The total mosquito population, $N_v(t)$ is stratified into questing and resting mosquitoes. Therefore, the mosquito population is subdivided into susceptible questing mosquitoes $S_q(t)$, infected questing mosquitoes $I_q(t)$, susceptible resting mosquitoes $S_r(t)$ and infected resting mosquitoes $I_r(t)$. Hence,

$$N_v(t) = S_q(t) + I_q(t) + S_r(t) + I_r(t).$$

The compartmental model assumes six interacting populations and is shown in Figure 3.1. The description of variables and parameters used in the model are as shown in Table 3.1 and Table 3.2, respectively.

Susceptible humans are recruited at the rate α_h into the population and increase due to addition of recovered humans from infection denoted by the term $\gamma_h I_h$. The susceptible humans are reduced due to contact with an infected questing mosquito through the term $b(T)\beta_h \frac{I_q}{N_h} S_h$ and by natural death rate through the term $\mu_h S_h$. For the infected human population, a proportion recover at a rate γ_h, others die naturally at a rate μ_h while others die due to infection at a rate δ_h. The proportion that recover at the rate γ_h returns back

to the susceptible population hence forming an SIS model for the human population.

For the vector population, susceptible resting vectors are recruited when type S_r or I_r vectors reproduce at the rate $\alpha_v(T,R)N_v$. A female mosquito only reproduce when it interacts with a human being at the human habitat, takes a blood meal, rests and then lays eggs at the mosquito breeding site. Eggs hatch into larvae which transform into pupae and later develop into adult vectors. Additional recruitment of susceptible resting vectors is through susceptible fed vectors that return from human habitats denoted by the term $p\alpha_s b(T)\frac{S_h}{N_h}S_q$. The population of susceptible resting vectors declines when a proportion of the vectors move to the questing population at the rate ω in search of a blood meal, when they die naturally, $\mu_v(T)$ and when they die due to contact with insecticides, δ_v. When a susceptible questing vector takes a blood from an infected human, it becomes a type I_r vector through the term $q\alpha_i b(T)\frac{I_h}{N_h}S_q$. Once a mosquito is infected, it remains infected till death. Therefore, infected resting vectors have additional recruitment from infected questing mosquitoes at the rate θ. The population declines when a proportion return to the infected questing population at the rate ω, when they die naturally, $\mu_v(T)$ and when they die due to contact with insecticides, δ_v.

Since the model system is studied under the presence of insecticide resistance, some of the malaria vectors develop resistant to insecticides at the rate ρ. If $\rho = 1$, then the total mosquito population will be resistant to insecticides. However, if $\rho = 0$, a proportion of the mosquito population will be sensitive to insecticides. The efficacy of insecticides on malaria vectors is determined by the rate ϵ while the death rate of the vectors is determined by the rate κ. Therefore, the proportion of mosquitoes sensitive to insecticides is denoted by the term $\epsilon\kappa(1-\rho)$.

The susceptible questing mosquitoes are reduced from the population due to death rate in three ways: the mosquitoes can die naturally at the rate $\mu_v(T)$, die due to contact with insecticides at the rate δ_v and die when a susceptible questing mosquito fail to successfully take a blood meal from either a susceptible or infectious human denoted by the terms $(1-p)\alpha_s b(T)\frac{S_h}{N_h}$ and $(1-q)\alpha_i b(T)\frac{I_h}{N_h}$, respectively. p is the probability of a susceptible questing mosquito successfully taking a blood meal from a susceptible human while q is the probability of a susceptible questing mosquito successfully taking a blood meal from

an infected human. Hence, the expression

$$\delta_q = \mu_v(T) + (1-p)\alpha_s b(T)\frac{S_h}{N_h} + (1-q)\alpha_i b(T)\frac{I_h}{N_h} + \delta_v.$$

Similarly, infected questing mosquitoes die naturally at the rate $\mu_v(T)$, due to contact with insecticides at the rate δ_v or when an infected questing mosquito fail to successfully take a blood meal from either a susceptible or infectious human denoted by the terms $(1-p_1)\alpha_s b(T)\frac{S_h}{N_h}$ and $(1-q_1)\alpha_i b(T)\frac{I_h}{N_h}$, respectively. Hence, the expression

$$\delta_{iq} = \mu_v(T) + (1-p_1)\alpha_s b(T)\frac{S_h}{N_h} + (1-q_1)\alpha_i b(T)\frac{I_h}{N_h} + \delta_v.$$

Additionally, the probability of an infected questing mosquito successfully taking a blood from a susceptible human is denoted by the term p_1 while the probability of it taking a blood meal from an infected human is q_1. Hence, the expression

$$\theta = \left(p_1\alpha_s\frac{S_h}{N_h} + q_1\alpha_i\frac{I_h}{N_h}\right)b(T).$$

The dynamics of malaria transmission in the presence of insecticide resistance and climatic variation is described by Figure 3.1 while state variables and parameter description are highlighted in Table 3.1 and Table 3.2, respectively.

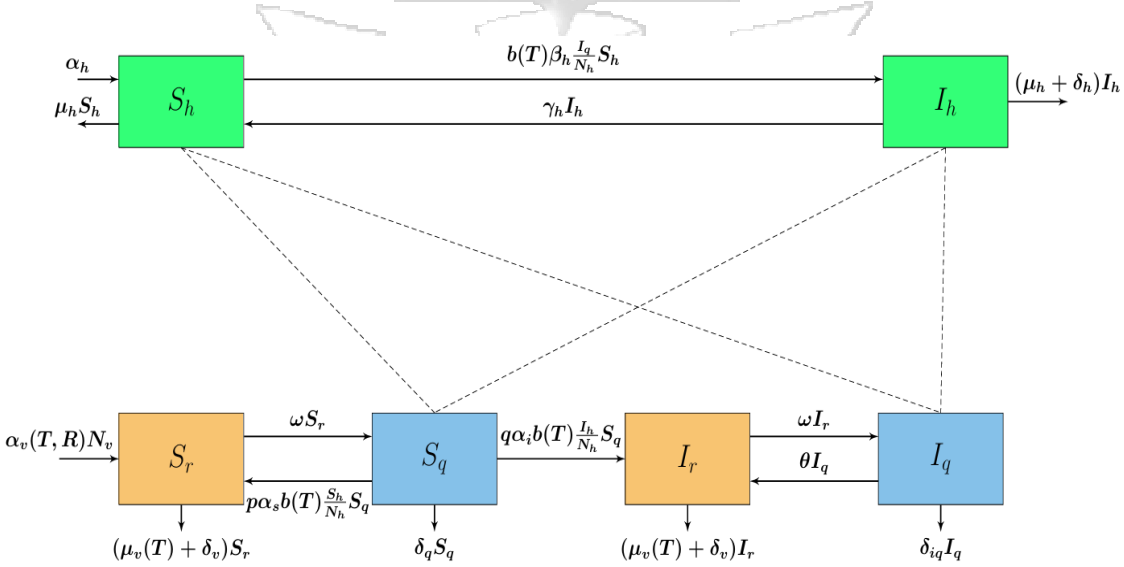

Figure 3.1: Flow diagram of malaria transmission under insecticide resistance

Table 3.1: Description of state variables

Variable	Description
S_h	Susceptible human population
I_h	Infected human population
S_r	Susceptible resting mosquito population
I_r	Infected resting mosquito population
S_q	Susceptible questing mosquito population
I_q	Infected questing mosquito population

Table 3.2: Description of parameters

Parameter	Description
α_h	Human recruitment rate
$b(T)$	Mosquito biting rate
β_h	Transition probability of susceptible humans to infectious humans
γ_h	Recovery rate amongst humans
μ_h	Natural human mortality rate
δ_h	Malaria induced human mortality rate
$\alpha_v(T, R)$	Mosquito birth rate
$\mu_v(T)$	Natural mortality rate mosquitoes
ω	Rate at which resting vectors are attracted to humans at the human habitat
p	Probability that a type S_q vector successfully takes a blood meal from a susceptible human
q	Probability that a type S_q vector successfully takes a blood meal from an infectious human
ϵ	Efficacy of insecticides
κ	Death rate of mosquitoes due to insecticides
ρ	Resistant acquisition ratio to the insecticides
α_s	Resting rate of susceptible mosquitoes
α_i	Resting rate of infected mosquitoes
p_1	Probability that a type I_q vector successfully takes a blood meal from a

Continued on next page

Table 3.2 – *Continued from previous page*

Parameter	Description
	susceptible human
q_1	Probability that a type I_q vector successfully takes a blood meal from an infectious human
B_E	Number of eggs laid per adult per oviposition
Γ_E	Daily survival probabilities of eggs
Γ_L	Daily survival probabilities of larvae
Γ_P	Daily survival probabilities of pupae
R_L	Rainfall limit beyond which breeding sites get flushed out and no immature stages survive

3.3 Mathematical Equations

Based on the above model description and assumptions, we have the following system of equations:

$$
\begin{aligned}
\frac{dS_h}{dt} &= \alpha_h + \gamma_h I_h - \left(b(T)\beta_h \frac{I_q}{N_h} + \mu_h \right) S_h, \\
\frac{dI_h}{dt} &= b(T)\beta_h \frac{I_q}{N_h} S_h - (\mu_h + \delta_h + \gamma_h) I_h, \\
\frac{dS_q}{dt} &= \omega S_r - \left(\mu_v(T) + \alpha_s b(T) \frac{S_h}{N_h} + \alpha_i b(T) \frac{I_h}{N_h} + \delta_v \right) S_q, \\
\frac{dI_q}{dt} &= \omega I_r - \left(\mu_v(T) + \alpha_s b(T) \frac{S_h}{N_h} + \alpha_i b(T) \frac{I_h}{N_h} + \delta_v \right) I_q, \\
\frac{dS_r}{dt} &= \alpha_v(T, R) N_v + p\alpha_s b(T) \frac{S_h}{N_h} S_q - (\omega + \mu_v(T) + \delta_v) S_r, \\
\frac{dI_r}{dt} &= q\alpha_i b(T) \frac{I_h}{N_h} S_q + \left(p_1 \alpha_s b(T) \frac{S_h}{N_h} + q_1 \alpha_i b(T) \frac{I_h}{N_h} \right) I_q - (\omega + \mu_v(T) + \delta_v) I_r.
\end{aligned}
\tag{1}
$$

where, $S_h > 0$, $I_h \geq 0$, $S_q \geq 0$, $I_q \geq 0$, $S_r > 0$,$I_r \geq 0$.

As highlighted in Abiodun et al. (2016, 2018), the mosquito oviposition rate is determined by the availability and conditions of mosquito breeding sites. Furthermore, other studies have indicated that some mosquitoes will not lay eggs if there is no breeding site available (Le Sueur and Sharp, 1988; Maharaj, 2003) and there is the possibility that female mosquitoes distribute their eggs among suitable and unoccupied containers (Wang et al.,

2011). Therefore, based on these facts, the mosquito birth rate of Parham and Michael (2010) will be adopted in this study, that is,

$$\alpha_v(R,T) = B_E\Gamma_E\Gamma_P\left(\frac{4\Gamma_L R(R_L-R)}{R_L^2}\right)\frac{(k_1T+k_2)e^{-(k_1T+k_2)}}{2(k_1T+k_2)+1},$$

where B_E is the number of eggs laid per adult mosquito per oviposition, Γ_E, Γ_L and Γ_P are the survival probabilities of eggs, larvae and pupae, respectively. R_L is the limit of rainfall beyond which breeding sites are flushed out and no immature stages of the mosquito survive. The values of k_1 and k_2 are 0.00554 and -0.06737, respectively.

To estimate the temperature dependent mortality rate of mosquitoes and biting rate, the expression of Ngarakana-Gwasira et al. (2016) and Paaijmans et al. (2013) will be adopted, that is,

$$\mu_v(T) = \tfrac{1}{c_1T^2+c_2T+c_3} \text{ and } b(T) = 0.000203T(T-11.7)\sqrt{(42.3-T)},$$

where, $c_1 = -0.03$, $c_2 = 1.13$, $c_3 = -4.4$.

3.4 Model Analysis

3.4.1 Positivity

Theorem 1. *For the given initial conditions of the model, the solutions of the model system remains positive for all $t > 0$.*

Proof. **Susceptible humans:** Taking the equation,

$$\begin{aligned}\frac{dS_h(t)}{dt} &= \alpha_h + \gamma_h I_h(t) - \left(b\beta_h\frac{I_q(t)}{N_h(t)} + \mu_h\right)S_h(t),\\ &\geq -\left(b\beta_h\frac{I_q(t)}{N_h(t)} + \mu_h\right)S_h(t).\end{aligned} \tag{2.1}$$

Putting like terms together and solving the above using separation of variables;

$$\begin{aligned}\frac{dS_h(t)}{S_h(t)} &\geq -\left(b\beta_h\frac{I_q(t)}{N_h(t)} + \mu_h\right)dt,\\ \int\frac{dS_h(t)}{S_h(t)} &\geq -\int_0^t\left(b\beta_h\frac{I_q(\tau)}{N_h(\tau)} + \mu_h\right)d\tau,\\ \ln|S_h| &\geq -\int_0^t\left(b\beta_h\frac{I_q(\tau)}{N_h(\tau)} + \mu_h\right)d\tau,\end{aligned}$$

Taking the exponential for both sides,

$$\begin{aligned} e^{\ln|S_h|} &\geq e^{-\int_0^t \left(b\beta_h \frac{I_q(\tau)}{N_h(\tau)}+\mu_h\right)d\tau}, \\ S_h(t) &\geq e^{-\int_0^t \left(b\beta_h \frac{I_q(\tau)}{N_h(\tau)}+\mu_h\right)d\tau}. \end{aligned} \tag{2.2}$$

The exponential part is greater that zero hence $S_h(t)$ is always positive, meaning: $S_h(t) > 0$ for all $t \to \infty$.

Infected humans: Taking the equation,

$$\begin{aligned} \frac{dI_h(t)}{dt} &= b\beta_h \frac{I_q(t)}{N_h(t)} S_h(t) - (\mu_h + \delta_h + \gamma_h) I_h(t), \\ &\geq -(\mu_h + \delta_h + \gamma_h) I_h(t). \end{aligned} \tag{2.3}$$

Putting like terms together and solving the above using separation of variables;

$$\begin{aligned} \frac{dI_h(t)}{I_h(t)} &\geq -(\mu_h + \delta_h + \gamma_h)dt, \\ \int \frac{dI_h(t)}{I_h(t)} &\geq -\int (\mu_h + \delta_h + \gamma_h)dt, \\ \ln|I_h(t)| &\geq -(\mu_h + \delta_h + \gamma_h)t + c_1, \end{aligned}$$

for constant c_1. Taking the exponential for both sides,

$$\begin{aligned} e^{\ln|I_h(t)|} &\geq e^{-(\mu_h+\delta_h+\gamma_h)t+c_1} = C_2 e^{-(\mu_h+\delta_h+\gamma_h)t}, \\ I_h(t) &\geq C_2 e^{-(\mu_h+\delta_h+\gamma_h)t}, \end{aligned}$$

where $C_2 = e^{c_1}$ is a constant. We substitute the initial condition $I_h(0) = I_0$, then

$$\begin{aligned} I_h(0) &\geq C_2 e^{-(\mu_h+\delta_h+\gamma_h)(0)} = I_0, \\ I_h(t) &\geq I_0 e^{-(\mu_h+\delta_h+\gamma_h)t}. \end{aligned} \tag{2.4}$$

Hence $C_2 = I_0$. The exponential part is greater that zero and $I_0 \geq 0$, hence $I_h(t)$ is always positive, meaning: $I_h(t) \geq 0$ for all $t \to \infty$.

Susceptible questing mosquitoes: Taking the equation,

$$\begin{aligned}\frac{dS_q(t)}{dt} &= \omega S_r(t) - \left(\mu_v + \alpha_s b\frac{S_h(t)}{N_h(t)} + \alpha_i b\frac{I_h(t)}{N_h(t)} + \delta_v\right) S_q(t),\\ &\geq -\left(\mu_v + \alpha_s b\frac{S_h(t)}{N_h(t)} + \alpha_i b\frac{I_h(t)}{N_h(t)} + \delta_v\right) S_q(t).\end{aligned} \tag{2.5}$$

Putting like terms together and solving the above using separation of variables;

$$\begin{aligned}\int \frac{dS_q(t)}{S_q(t)} &\geq -\int_0^t \left(\mu_v + \alpha_s b\frac{S_h(\tau)}{N_h(\tau)} + \alpha_i b\frac{I_h(\tau)}{N_h(\tau)} + \delta_v\right) d\tau,\\ \ln|S_q(t)| &\geq -\int_0^t \left(\mu_v + \alpha_s b\frac{S_h(\tau)}{N_h(\tau)} + \alpha_i b\frac{I_h(\tau)}{N_h(\tau)} + \delta_v\right) d\tau,\end{aligned}$$

Taking the exponential for both sides,

$$\begin{aligned}e^{\ln|S_q(t)|} &\geq e^{-\int_0^t \left(\mu_v + \alpha_s b\frac{S_h(\tau)}{N_h(\tau)} + \alpha_i b\frac{I_h(\tau)}{N_h(\tau)} + \delta_v\right) d\tau},\\ S_q(t) &\geq e^{-\int_0^t \left(\mu_v + \alpha_s b\frac{S_h(\tau)}{N_h(\tau)} + \alpha_i b\frac{I_h(\tau)}{N_h(\tau)} + \delta_v\right) d\tau}.\end{aligned} \tag{2.6}$$

The exponential is greater than zero and hence $S_q(t)$ is always positive, meaning: $S_q(t) \geq 0$ for all $t \to \infty$.

Infected questing mosquitoes: Taking the equation,

$$\begin{aligned}\frac{dI_q(t)}{dt} &= \omega I_r(t) - \left(\mu_v + \alpha_s b\frac{S_h(t)}{N_h(t)} + \alpha_i b\frac{I_h(t)}{N_h(t)} + \delta_v\right) I_q(t),\\ &\geq -\left(\mu_v + \alpha_s b\frac{S_h(t)}{N_h(t)} + \alpha_i b\frac{I_h(t)}{N_h(t)} + \delta_v\right) I_q(t).\end{aligned} \tag{2.7}$$

Putting like terms together and solving the above using separation of variables;

$$\begin{aligned}\int \frac{dI_q(t)}{I_q(t)} &\geq -\int_0^t \left(\mu_v + \alpha_s b\frac{S_h(\tau)}{N_h(\tau)} + \alpha_i b\frac{I_h(\tau)}{N_h(\tau)} + \delta_v\right) d\tau,\\ \ln|I_q(t)| &\geq -\int_0^t \left(\mu_v + \alpha_s b\frac{S_h(\tau)}{N_h(\tau)} + \alpha_i b\frac{I_h(\tau)}{N_h(\tau)} + \delta_v\right) d\tau,\end{aligned}$$

Taking the exponential for both sides,

$$\begin{aligned}e^{\ln|I_q(t)|} &\geq e^{-\int_0^t \left(\mu_v + \alpha_s b\frac{S_h(\tau)}{N_h(\tau)} + \alpha_i b\frac{I_h(\tau)}{N_h(\tau)} + \delta_v\right) d\tau},\\ I_q(t) &\geq e^{-\int_0^t \left(\mu_v + \alpha_s b\frac{S_h(\tau)}{N_h(\tau)} + \alpha_i b\frac{I_h(\tau)}{N_h(\tau)} + \delta_v\right) d\tau}.\end{aligned} \tag{2.8}$$

The exponential is greater than zero and hence $I_q(t)$ is always positive, meaning: $I_q(t) \geq 0$ for all $t \to \infty$.

Susceptible resting mosquitoes: Taking the equation,

$$\begin{aligned} \frac{dS_r(t)}{dt} &= \alpha_v N_v(t) + p\alpha_s b \frac{S_h(t)}{N_h(t)} S_q(t) - (\omega + \mu_v + \delta_v) S_r(t), \\ &\geq -(\omega + \mu_v + \delta_v) S_r(t). \end{aligned} \tag{2.9}$$

Putting like terms together and solving the above using separation of variables;

$$\begin{aligned} \frac{dS_r(t)}{S_r(t)} &\geq -(\omega + \mu_v + \delta_v) dt, \\ \int \frac{dS_r(t)}{S_r(t)} &\geq -\int (\omega + \mu_v + \delta_v) dt, \\ \ln |S_r(t)| &\geq -(\omega + \mu_v + \delta_v) t + c_3, \end{aligned}$$

for constant c_3.

Taking the exponential for both sides,

$$\begin{aligned} e^{\ln |S_r(t)|} &\geq e^{-(\omega+\mu_v+\delta_v)t + c_3} = C_4 e^{-(\omega+\mu_v+\delta_v)t}, \\ S_r(t) &\geq C_4 e^{-(\omega+\mu_v+\delta_v)t}, \end{aligned}$$

where $C_4 = e^{c_3}$ is a constant.

At t=0, $S_r(0) \geq C_4$ therefore,

$$S_r(t) \geq S_r(0) e^{-(\omega+\mu_v+\delta_v)t}. \tag{2.10}$$

The exponential is greater than zero and hence $S_r(t)$ is always positive, meaning: $S_r(t) > 0$ for all $t \to \infty$.

Infected resting mosquitoes: Taking the equation,

$$\begin{aligned} \frac{dI_r(t)}{dt} &= q\alpha_i b \frac{I_h(t)}{N_h(t)} S_q(t) + \left(p_1 \alpha_s b \frac{S_h(t)}{N_h(t)} + q_1 \alpha_i b \frac{I_h(t)}{N_h(t)} \right) I_q(t) - (\omega + \mu_v + \delta_v) I_r(t), \\ &\geq -(\omega + \mu_v + \delta_v) I_r(t). \end{aligned} \tag{2.11}$$

Putting like terms together and solving the above using separation of variables;

$$\begin{aligned}\frac{dI_r(t)}{I_r(t)} &\geq -(\omega+\mu_v+\delta_v)dt,\\ \int\frac{dI_r(t)}{I_r(t)} &\geq -\int(\omega+\mu_v+\delta_v)dt,\\ \ln|I_r(t)| &\geq -(\omega+\mu_v+\delta_v)t+c_5,\end{aligned}$$

for constant c_5.Taking the exponential for both sides,

$$\begin{aligned}e^{\ln|I_r(t)|} &\geq e^{-(\omega+\mu_v+\delta_v)t+c_5} = C_6e^{-(\omega+\mu_v+\delta_v)t},\\ I_r(t) &\geq C_6e^{-(\omega+\mu_v+\delta_v)t},\end{aligned}$$

where $C_6 = e^{c_5}$ is a constant.
At t=0, $I_r(0) \geq C_6$ therefore,

$$I_r(t) \geq I_r(0)e^{-(\omega+\mu_v+\delta_v)t}. \tag{2.12}$$

The exponential is greater than zero and $I_r(t) \geq 0$, hence $I_r(t)$ is always positive, meaning: $I_r(t) \geq 0$ for all $t \to \infty$. □

3.4.2 Boundedness

Boundedness ensures population sizes within each compartment cannot grow indefinitely or exceed reasonable and feasible range. From this the given theorem is arrived at:

Theorem 2. *The solutions of a model system (1) with initial conditions given are bounded in a positive region,*

$$\begin{aligned}&\mathcal{D} = \mathcal{D}_h + \mathcal{D}_v \in \mathbb{R}^6_+ \text{ with}\\ &\mathcal{D}_h = \{(S_h, I_h) \in \mathbb{R}^2_+ : 0 < S_h + I_h < \frac{\alpha_h}{\mu_h}\} \text{ and}\\ &\mathcal{D}_v = \{(S_q, I_q, S_r, I_r) \in \mathbb{R}^4_+ : 0 < S_q + I_q + S_r + I_r < \frac{1}{\mu_v+\delta_v-\alpha_v}\}\end{aligned}$$

for any time $t \geq 0$.

Proof. Let $N_h(t) = S_h(t) + I_h(t)$ be the total human population and $N_v(t) = S_q(t) +$

$I_q(t) + S_r(t) + I_r(t)$ be the total mosquito population. To show that the solutions of the model system are bounded we proceed as follows:

$$\frac{dN_h}{dt} = \frac{dS_h}{dt} + \frac{dI_h}{dt}. \tag{3.1}$$

$$\begin{aligned}
\frac{dN_h}{dt} &= \alpha_h + \gamma_h I_h - \left(b\beta_h \frac{I_q}{N_h} + \mu_h\right) S_h + b\beta_h \frac{I_q}{N_h} S_h - (\mu_h + \delta_h + \gamma_h) I_h, \\
&= \alpha_h - \mu_h S_h - \mu_h I_h - \delta_h I_h, \\
&= \alpha_h - \mu_h (S_h + I_h) - \delta_h I_h, \\
&= \alpha_h - \mu_h N_h - \delta_h I_h.
\end{aligned}$$

Assuming that there is no disease in the population

$$\begin{aligned}
\frac{dN_h}{dt} &\leq \alpha_h - \mu_h N_h, \\
\frac{dN_h}{dt} + \mu_h N_h &\leq \alpha_h.
\end{aligned}$$

Integrating factor $= e^{\int \mu_h dt} = e^{\mu_h t}$.

Thus,

$$\begin{aligned}
e^{\mu_h t}\left[\frac{dN_h}{dt} + \mu_h N_h\right] &\leq \alpha_h e^{\mu_h t}, \\
\frac{d}{dt}\left[N_h e^{\mu_h t}\right] &\leq \alpha_h e^{\mu_h t}, \\
N_h e^{\mu_h t} &\leq \int \alpha_h e^{\mu_h t} dt, \\
N_h e^{\mu_h t} &\leq \frac{\alpha_h}{\mu_h} e^{\mu_h t} + c, \\
N_h &\leq \frac{\alpha_h}{\mu_h} + c e^{-\mu_h t}.
\end{aligned}$$

$$\text{As } t \to \infty, \quad N_h(t) \leq \frac{\alpha_h}{\mu_h}. \tag{3.2}$$

Hence, $N_h(t) \leq \frac{\alpha_h}{\mu_h}$, $\forall\ t > 0$.

For the mosquito population where $N_v(t) = S_q(t) + I_q(t) + S_r(t) + I_r(t)$ can also be shown to be bounded as follows:

$$\begin{aligned}
\frac{dN_v(t)}{dt} &= \frac{d[S_q(t) + I_q(t) + S_r(t) + I_r(t)]}{dt}. \\
&= \omega S_r - \left(\mu_v + \alpha_s b\frac{S_h}{N_h} + \alpha_i b\frac{I_h}{N_h} + \delta_v\right) S_q \\
&+ \omega I_r - \left(\mu_v + \alpha_s b\frac{S_h}{N_h} + \alpha_i b\frac{I_h}{N_h} + \delta_v\right) I_q \\
&+ \alpha_v N_v + p\alpha_s b\frac{S_h}{N_h} S_q - (\omega + \mu_v + \delta_v) S_r \\
&+ q\alpha_i b\frac{I_h}{N_h} S_q + \left(p_1\alpha_s b\frac{S_h}{N_h} + q_1\alpha_i b\frac{I_h}{N_h}\right) I_q \\
&- (\omega + \mu_v + \delta_v) I_r, \\
&= \alpha_v N_v - \mu_v N_v - \delta_v N_v + (p-1)\alpha_s b\frac{S_h}{N_h} S_q \\
&+ (q-1)\alpha_i b\frac{I_h}{N_h} S_q + (p_1 - 1)\alpha_s b\frac{S_h}{N_h} I_q \\
&+ (q_1 - 1)\alpha_i b\frac{I_h}{N_h} I_q.
\end{aligned}$$

Assuming there is no disease in the population,

$$\begin{aligned}
\frac{dN_v(t)}{dt} &\leq \alpha_v N_v - \mu_v N_v - \delta_v N_v, \\
&\leq -(\mu_v + \delta_v - \alpha_v) N_v.
\end{aligned}$$

By letting $\psi = \mu_v + \delta_v - \alpha_v$ we have

$$\frac{dN_v(t)}{dt} + \psi N_v \leq 1. \tag{3.3}$$

Integrating factor $= e^{\int \psi dt} = e^{\psi t}$.

Thus,

$$\begin{aligned}
e^{\psi t}[\frac{dN_v(t)}{dt} + \psi N_v] &\leq e^{\psi t}, \\
\frac{d}{dt}[N_v e^{\psi t}] &\leq e^{\psi t}, \\
N_v e^{\psi t} &\leq \int e^{\psi t} dt, \\
N_v e^{\psi t} &\leq \frac{e^{\psi t}}{\psi} + c,
\end{aligned}$$

$$N_v \leq \frac{1}{\psi} + ce^{-\psi t}.$$

$$\text{As } t \to \infty, \quad N_v(t) \leq \frac{1}{\psi}. \tag{3.4}$$

Replacing the value of ψ in equation (3.4) yields:

$$N_v(t) \leq \frac{1}{\mu_v + \delta_v - \alpha_v}. \tag{3.5}$$

Therefore, $N_v(t)$ is bounded in the region $N_v(t) \leq \frac{1}{\mu_v+\delta_v-\alpha_v}$, $\forall\ t > 0$.
Therefore, every solution of the model equation is bounded by the region $\mathcal{D}$. □

3.5 Disease Free Equilibrium

The disease free equilibrium is obtained by setting the system of differential equations to zero. Setting all infected classes to zero, we have the disease free equilibrium as;

$$E_0 = \left(\frac{\alpha_h}{\mu_h}, 0, m_1, 0, m_2, 0\right).$$

where,

$$m_1 = \frac{\omega\mu_h N_h \alpha_v N_v}{(\omega + \mu_v + \delta_v)(\mu_v\mu_h N_h + \alpha_s b\alpha_h + \delta_v\mu_h N_h) - \omega p\alpha_s b\alpha_h},$$
$$m_2 = \frac{\alpha_v N_v}{\omega + \mu_v + \delta_v} + \frac{p\alpha_s b\alpha_h m_1}{\mu_h N_h(\omega + \mu_v + \delta_v)}.$$

3.6 Basic Reproduction Number

The basic reproduction number was computed using the next generation matrix approach. The matrix F of new infections and matrix V showing the transfer of infections from one compartment to the other were generated.

$$\mathcal{F} = \begin{bmatrix} b\beta_h \frac{I_q}{N_h} S_h \\ 0 \\ q\alpha_i b \frac{I_h}{N_h} S_q \end{bmatrix}, \tag{4.1}$$

$$\mathcal{V} = \begin{bmatrix} (\mu_h + \delta_h + \gamma_h) I_h \\ -\omega I_r + \left(\mu_v + \alpha_s b \frac{S_h}{N_h} + \alpha_i b \frac{I_h}{N_h} + \delta_v\right) I_q \\ -\left(p_1 \alpha_s b \frac{S_h}{N_h} + q_1 \alpha_i b \frac{I_h}{N_h}\right) I_q + (\omega + \mu_v + \delta_v) I_r \end{bmatrix}. \tag{4.2}$$

The Jacobian matrix of F and V is given by

$$J_F = F = \begin{bmatrix} 0 & b\beta_h \frac{S_h}{N_h} & 0 \\ 0 & 0 & 0 \\ q\alpha_i b \frac{S_q}{N_h} & 0 & 0 \end{bmatrix} \text{ and}$$

$$J_V = V = \begin{bmatrix} \mu_h + \delta_h + \gamma_h & 0 & 0 \\ \alpha_i \frac{b}{N_h} I_q & \left(\mu_v + \alpha_s b \frac{S_h}{N_h} + \alpha_i b \frac{I_h}{N_h} + \delta_v\right) & -\omega \\ -q_1 \alpha_i b \frac{I_q}{N_h} & -\left(p_1 \alpha_s b \frac{S_h}{N_h} + q_1 \alpha_i b \frac{I_h}{N_h}\right) & (\omega + \mu_v + \delta_v) \end{bmatrix}.$$

At the disease free equilibrium we have

$$J_F = F = \begin{bmatrix} 0 & b\beta_h \frac{\alpha_h}{\mu_h N_h} & 0 \\ 0 & 0 & 0 \\ q\alpha_i b \frac{m_1}{N_h} & 0 & 0 \end{bmatrix} \text{ and} \tag{4.3}$$

$$J_V = V = \begin{bmatrix} \mu_h + \delta_h + \gamma_h & 0 & 0 \\ 0 & \left(\mu_v + \alpha_s b \frac{\alpha_h}{\mu_h N_h} + \delta_v\right) & -\omega \\ 0 & -p_1 \alpha_s b \frac{S_h}{N_h} & \omega + \mu_v + \delta_v \end{bmatrix}. \tag{4.4}$$

$$V^{-1} = \begin{bmatrix} \frac{1}{\gamma_h+\delta_h+\mu_h} & 0 & 0 \\ 0 & A & B \\ 0 & C & D \end{bmatrix}. \tag{4.5}$$

where,

$$A = \frac{\delta_v + \mu_v + \omega}{(\delta_v + \mu_v + \omega)\left(\frac{b\alpha_h\alpha_s}{\mu_h N_h} + \delta_v + \mu_v\right) - \frac{bp_1\omega\alpha_h\alpha_s}{\mu_h N_h}},$$

$$B = \frac{\omega(\gamma_h + \delta_h + \mu_h)}{(\gamma_h + \delta_h + \mu_h)\left((\delta_v + \mu_v + \omega)\left(\frac{b\alpha_h\alpha_s}{\mu_h N_h} + \delta_v + \mu_v\right) - \frac{bp_1\omega\alpha_h\alpha_s}{\mu_h N_h}\right)},$$

$$C = \frac{bp_1\alpha_h\alpha_s}{\mu_h N_h\left((\delta_v + \mu_v + \omega)\left(\frac{b\alpha_h\alpha_s}{\mu_h N_h} + \delta_v + \mu_v\right) - \frac{bp_1\omega\alpha_h\alpha_s}{\mu_h N_h}\right)},$$

$$D = \frac{\frac{b\alpha_h\alpha_s}{\mu_h N_h} + \delta_v + \mu_v}{(\delta_v + \mu_v + \omega)\left(\frac{b\alpha_h\alpha_s}{\mu_h N_h} + \delta_v + \mu_v\right) - \frac{bp_1\omega\alpha_h\alpha_s}{\mu_h N_h}}.$$

The next generation matrix which is the product of F and V^{-1} is given by:

$$FV^{-1} = \begin{bmatrix} 0 & E & F \\ 0 & 0 & 0 \\ G & 0 & 0 \end{bmatrix}. \tag{4.6}$$

where,

$$E = \frac{b\alpha_h\beta_h(\delta_v + \mu_v + \omega)}{\mu_h N_h\left((\delta_v + \mu_v + \omega)\left(\frac{b\alpha_h\alpha_s}{\mu_h N_h} + \delta_v + \mu_v\right) - \frac{bp_1\omega\alpha_h\alpha_s}{\mu_h N_h}\right)},$$

$$F = \frac{b\alpha_h\beta_h\omega(\gamma_h + \delta_h + \mu_h)}{\mu_h N_h(\gamma_h + \delta_h + \mu_h)\left((\delta_v + \mu_v + \omega)\left(\frac{b\alpha_h\alpha_s}{\mu_h N_h} + \delta_v + \mu_v\right) - \frac{bp_1\omega\alpha_h\alpha_s}{\mu_h N_h}\right)},$$

$$G = \frac{bq\alpha_i\omega\mu_h\alpha_v N_v}{(\gamma_h + \delta_h + \mu_h)((\delta_v + \mu_v + \omega)(b\alpha_h\alpha_s + N_h\delta_v\mu_h + \mu_h N_h\mu_v) - b\alpha_h\omega\lambda\alpha_s)}.$$

The basic reproduction number R_0 of the next-generation matrix FV^{-1} is given by:

$$R_0 = \sqrt{\frac{R_*}{R_{**}}}. \tag{4.7}$$

where,

$$R_* = (b)^2 q\omega^2 \alpha_h \alpha_v \alpha_i \beta_h \mu_h N_v.$$

$$R_{**} = (\mu_h + \gamma_h + \delta_h)(b\alpha_h\alpha_s(\delta_v + \omega(1-p_1) + \mu_v) + \mu_h(\delta_v + \mu_v)(\delta_v + \omega + \mu_v)N_h)((\delta_v + \omega + \mu_v)(b\alpha_h\alpha_s + (\delta_v\mu_h + \mu_h\mu_v)N_h) - b\alpha_h\omega p\alpha_s).$$

If $R_0 < 1$ it implies that malaria infection will eventually reduce in the population but if $R_0 > 1$ it implies that malaria disease will persist in the population.

3.7 Stability Analysis of Disease Free Equilibrium

3.7.1 Local Stability of Disease Free Equilibrium

The local stability analysis of the disease free equilibrium point (DFE) of the model is determined by finding the Jacobian matrix and its eigenvalues. An equilibrium point is locally asymptotically stable if all the eigenvalues of the jacobian matrix at that point are negative. The general Jacobian matrix of the model is:

$$J = \begin{bmatrix} \frac{-b\beta_h I_q}{N_h} + \mu_h & \gamma_h & 0 & -\frac{b\beta_h S_h}{N_h} & 0 & 0 \\ \frac{b\beta_h I_q}{N_h} & -(\mu_h + \delta_h + \gamma_h) & 0 & \frac{b\beta_h S_h}{N_h} & 0 & 0 \\ -\frac{\alpha_s b S_q}{N_h} & -\frac{\alpha_i b S_q}{N_h} & C_1 & 0 & \omega & 0 \\ -\frac{\alpha_s b I_q}{N_h} & -\frac{\alpha_i b I_q}{N_h} & 0 & C_1 & 0 & \omega \\ \frac{p\alpha_s b S_q}{N_h} & 0 & \frac{p\alpha_s b S_h}{N_h} & 0 & C_2 & 0 \\ \frac{p_1\alpha_s b I_q}{N_h} & C_3 & \frac{q\alpha_i b I_h}{N_h} & C_4 & 0 & C_2 \end{bmatrix} \tag{5.1}$$

where;

$$C_1 = -\left(\mu_v + \frac{\alpha_s b S_h}{N_h} + \frac{\alpha_i b I_h}{N_h} + \delta_v\right),$$

$$C_2 = -(\omega + \mu_v + \delta_v),$$

$$C_3 = \frac{q\alpha_i b S_q}{N_h} + \frac{q_1\alpha_i b I_q}{N_h},$$

$$C_4 = \frac{p_1\alpha_s b S_h}{N_h} + \frac{q_1\alpha_i b I_h}{N_h}.$$

The jacobian at the disease free equilibrium is given as

$$J_{E_0} = \begin{bmatrix} -\mu_h & \gamma_h & 0 & -\frac{b\beta_h\alpha_h}{\mu_h N_h} & 0 & 0 \\ 0 & -(\mu_h+\delta_h+\gamma_h) & 0 & \frac{b\beta_h\alpha_h}{\mu_h N_h} & 0 & 0 \\ -\frac{\alpha_s b m_1}{N_h} & -\frac{\alpha_i b m_1}{N_h} & C_5 & 0 & \omega & 0 \\ 0 & 0 & 0 & C_5 & 0 & \omega \\ \frac{p\alpha_s b m_1}{N_h} & 0 & \frac{p\alpha_s b\alpha_h}{\mu_h N_h} & 0 & C_6 & 0 \\ 0 & \frac{q\alpha_i b m_1}{N_h} & 0 & \frac{p_1\alpha_s b\alpha_h}{\mu_h N_h} & 0 & C_6 \end{bmatrix}. \tag{5.2}$$

where;

$$C_5 = -\left(\mu_v + \alpha_s b\frac{\alpha_h}{\mu_h N_h} + \delta_v\right),$$
$$C_6 = -(\omega + \mu_v + \delta_v).$$

In the Jacobian matrix (5.2), it is clear that the first and second eigenvalues are $\lambda_1 = \lambda_2 = C_6 = -(\omega + \mu_v + \delta_v)$ since the fifth and sixth rows and columns of matrix (5.2) is a diagonal matrix. Upon deleting the fifth and sixth rows and columns, matrix (5.2) is reduced to:

$$J_{E_0} = \begin{bmatrix} -\mu_h & \gamma_h & 0 & -\frac{b\beta_h\alpha_h}{\mu_h N_h} \\ 0 & -(\mu_h+\delta_h+\gamma_h) & 0 & \frac{b\beta_h\alpha_h}{\mu_h N_h} \\ -\frac{\alpha_s b m_1}{N_h} & -\frac{\alpha_i b m_1}{N_h} & C_5 & 0 \\ 0 & 0 & 0 & C_5 \end{bmatrix}, \tag{5.3}$$

where;

$$C_5 = -\left(\mu_v + \frac{b\alpha_s\alpha_h}{\mu_h N_h} + \delta_v\right).$$

The third and fourth rows and columns of matrix (5.3) is a diagonal matrix, therefore the third and fourth eigenvalues are $\lambda_3 = C_5 = -(\mu_v + \frac{b\alpha_s\alpha_h}{\mu_h N_h} + \delta_v)$ and $\lambda_4 = C_5 = -(\mu_v + \frac{b\alpha_h\alpha_s}{\mu_h N_h} + \delta_v)$. Matrix (5.3) is therefore further reduced by deleting the third and

fourth rows and columns.

$$J_{E_0} = \begin{bmatrix} -\mu_h & \gamma_h \\ 0 & -(\mu_h + \delta_h + \gamma_h) \end{bmatrix}. \tag{5.4}$$

Matrix (5.4) is an upper triangular matrix and hence $\lambda_5 = -\mu_h$ and $\lambda_6 = -(\mu_h + \delta_h + \gamma_h)$. Since all the eigenvalues of the Jacobian matrix (5.2) are all negative:

$$\lambda_1 = -(\omega + \mu_v + \delta_v); \lambda_2 = -(\omega + \mu_v + \delta_v); \lambda_3 = -\left(\mu_v + \frac{b\alpha_s\alpha_h}{\mu_h N_h} + \delta_v\right)$$
$$\lambda_4 = -\left(\mu_v + \frac{b\alpha_s\alpha_h}{\mu_h N_h} + \delta_v\right); \lambda_5 = -\mu_h; \lambda_6 = -(\mu_h + \delta_h + \gamma_h).$$

The disease free equilibrium point is therefore locally asymptotically stable.

3.7.2 Global Stability Analysis of Disease Free Equilibrium

The global stability of disease free equilibrium point of the model system is assessed by utilizing Castillo–Chavez approach (Castillo-Chavez et al. (2002)). The model system (1) was first written in the form:

$$\begin{aligned} \frac{dX_1}{dt} &= H(X_1, X_2), \\ \frac{dX_2}{dt} &= G(X_1, X_2), \end{aligned} \tag{6.1}$$

where X_1 denotes the states of human and mosquito compartments that are not infected and do not transmit malaria disease while X_2 represents the states of human and mosquito compartments involved in malaria disease transmission. Therefore,

$$X_1 = (S_h, S_q, S_r), X_2 = (I_h, I_q, I_r), \text{ and } E^0 = (X_1^0, 0). \tag{6.2}$$

Based on Castillo–Chavez approach (Castillo-Chavez et al. (2002)), global stability at disease free equilibrium point exists if the following two conditions are met:

1. If $\frac{dX_1}{dt} = H(X_1, 0)$, X_1^0 is globally asymptotically stable.
2. $G(X_1, X_2) = AX_2^T - \hat{G}(X_1, X_2)$, $\hat{G}(X_1, X_2) \geq 0$ for $(X_1, X_2) \in \Omega$.

In the second condition, $A = D_{X_2}G(X_1^0, 0)$ is an M-matrix, that is the off diagonal entries of the matrix are non negative and Ω is a feasible region.

Lemma 1. *For $R_0 < 1$, the equilibrium point $E_0 = (X_1^0, 0)$ of the model system (1) is globally asymptotically stable, if the above conditions are satisfied (Castillo-Chavez et al. (2002)).*

Theorem 3. *If $R_0 < 1$, then the model system (1) is globally asymptotically stable at disease-free equilibrium E_0 and unstable otherwise.*

Proof. Let $X_1 = (S_h, S_q, S_r)$; $X_2 = (I_h, I_q, I_r)$ and $E_0 = X_1^0$, where

$$X_1^0 = \left(\frac{\alpha_h}{\mu_h}, m_1, m_2\right), \tag{6.3}$$

and

$$m_1 = \frac{\omega\mu_h N_h \alpha_v N_v}{(\omega+\mu_v+\delta_v)(\mu_v\mu_h N_h + \alpha_s b\alpha_h + \delta_v\mu_h N_h) - \omega p\alpha_s b\alpha_h},$$
$$m_2 = \frac{\alpha_v N_v}{\omega+\mu_v+\delta_v} + \frac{p\alpha_s b\alpha_h m_1}{\mu_h N_h(\omega+\mu_v+\delta_v)}.$$

From the model system (1), we have

$$\frac{dX_1}{dt} = H(X_1, X_2),$$

$$\frac{dX_1}{dt} = \begin{pmatrix} \alpha_h + \gamma_h I_h - \left(\frac{b\beta_h I_q}{N_h} + \mu_h\right) S_h \\ \omega S_r - \left(\mu_v + \frac{b\alpha_s S_h}{N_h} + \frac{b\alpha_i I_h}{N_h} + \delta_v\right) S_q \\ \alpha_v N_v + \frac{p\alpha_s b S_h S_q}{N_h} - (\omega+\mu_v+\delta_v) S_r \end{pmatrix}. \tag{6.4}$$

For $S_h = S_h^0, S_q = S_q^0, S_r = S_r^0$ and $H(X_1, 0) = 0$, we get

$$H(X_1, 0) = \begin{pmatrix} \alpha_h - \mu_h S_h \\ \omega S_r - \left(\mu_v + \frac{b\alpha_s S_h}{N_h} + \delta_v\right) S_q \\ \alpha_v N_v + \frac{p\alpha_s b S_h S_q}{N_h} - (\omega+\mu_v+\delta_v) S_r \end{pmatrix} = 0. \tag{6.5}$$

From equation (6.5), as $t \to \infty$, $X_1 \to X_1^0$. Therefore, $X_1 = X_1^0$ is globally asymptotically stable.

From the second condition,

$G(X_1, X_2) = AX_2 - \hat{G}(X_1, X_2)$

$A = D_{X_2} G(X_1^0, 0)$

$$A = \begin{pmatrix} -(\mu_h + \delta_h + \gamma_h) & \frac{b\beta_h S_h^0}{N_h} & 0 \\ 0 & -\left(\mu_v + \frac{\alpha_s b S_h^0}{N_h} + \delta_v\right) & \omega \\ \frac{q\alpha_i b S_q^0}{N_h} & \frac{p_1 \alpha_s b S_h^0}{N_h} & -(\omega + \mu_v + \delta_v) \end{pmatrix}.$$

$$G(X_1, X_2) = \begin{pmatrix} \frac{b\beta_h I_q S_h}{N_h} - (\mu_h + \delta_h + \gamma_h) I_h \\ \omega I_r - \left(\mu_v + \frac{\alpha_s b S_h}{N_h} + \frac{\alpha_i b I_h}{N_h} + \delta_v\right) I_q \\ \frac{q\alpha_i b I_h S_q}{N_h} + (\frac{p_1 \alpha_s b S_h}{N_h} + \frac{q_1 \alpha_i b I_h}{N_h}) I_q - (\omega + \mu_v + \delta_v) I_r \end{pmatrix}$$

$$\hat{G}(X_1, X_2) = \begin{pmatrix} 0 \\ 0 \\ 0 \end{pmatrix}.$$

$G(X_1, X_2) = AX_2 - \hat{G}(X_1, X_2)$ is therefore given by

$$G(X_1, X_2) = \begin{pmatrix} -(\mu_h + \delta_h + \gamma_h) & \frac{b(T)\beta_h S_h^0}{N_h} & 0 \\ 0 & -\left(\mu_v + \frac{\alpha_s b S_h^0}{N_h} + \delta_v\right) & \omega \\ \frac{q\alpha_i b S_q^0}{N_h} & \frac{p_1 \alpha_s b S_h^0}{N_h} & -(\omega + \mu_v + \delta_v) \end{pmatrix} \begin{pmatrix} I_h \\ I_w \\ I_v \end{pmatrix} - \begin{pmatrix} 0 \\ 0 \\ 0 \end{pmatrix}$$

$\hat{G}(X_1, X_2) \geq 0$ and A is an M-matrix since the off diagonal entries are non negative. Therefore, since both the two conditions have been proved, by lemma 1 the disease free equilibrium point E^0 is globally asymptotically stable. □

3.8 Endemic Equilibrium Point

Endemic equilibrium is achieved when $R_0 > 1$. The RHS of the model system was equated to zero and solved for all state variables, $S_h, I_h, S_q, I_q, S_r, I_r$. The model system

was solved in mathematica software and the steady states obtained for E_1 are:

$$E_1 = (S_h^*, I_h^*, S_q^*, I_q^*, S_r^*, I_r^*),$$

where,

$$\begin{aligned}
S_h^* &= \frac{(\alpha_h + \gamma_h I_h)\, N_h}{b\beta_h I_q + \mu_h N_h}, \\
I_h^* &= \frac{b\beta_h S_h I_q}{(\gamma_h + \delta_h + \mu_h)\, N_h}, \\
S_q^* &= \frac{\omega S_r N_h}{b\alpha_i I_h + b\alpha_s S_h + \delta_v N_h + \mu_v N_h}, \\
I_q^* &= \frac{\omega I_r N_h}{b\alpha_i I_h + b\alpha_s S_h + \delta_v N_h + \mu_v N_h}, \\
S_r^* &= \frac{bp\alpha_s S_h S_q + \alpha_v N_v N_h}{(\delta_v + \mu_v + \omega)\, N_h} \text{ and} \\
I_r^* &= \frac{bq_1\alpha_i I_h I_q + bq\alpha_i I_h S_q + bp_1\alpha_s S_h I_q}{(\delta_v + \mu_v + \omega)\, N_h}.
\end{aligned} \tag{7}$$

Therefore, there exists a unique endemic equilibrium point at $R_0 > 1$ and no endemic equilibrium when $R_0 < 1$.

3.9 Optimal Control Problem

In this section, the model system (1) is reformulated by incorporating three control variables: personal protection such as use of insecticide treated nets, u_1, antimalarial treatment, u_2 and use of vaccination to prevent malaria, u_3. The reformulated model with the presence of controls is given as:

$$\begin{aligned}
\frac{dS_h}{dt} &= (1-u_3)\alpha_h + (u_2+\gamma_h)I_h - \left((1-u_1)b\beta_h\frac{I_q}{N_h} + \mu_h\right)S_h, \\
\frac{dI_h}{dt} &= (1-u_1)b\beta_h\frac{I_q}{N_h}S_h - (\mu_h + \delta_h + (u_2+\gamma_h)I_h, \\
\frac{dS_q}{dt} &= \omega S_r - \left(\mu_v + (1-u_1)\alpha_s b\frac{S_h}{N_h} + (1-u_1)\alpha_i b\frac{I_h}{N_h} + \delta_v\right)S_q, \\
\frac{dI_q}{dt} &= \omega I_r - \left(\mu_v + (1-u_1)\alpha_s b\frac{S_h}{N_h} + (1-u_1)\alpha_i b\frac{I_h}{N_h} + \delta_v\right)I_q, \\
\frac{dS_r}{dt} &= \alpha_v N_v + (1-u_1)p\alpha_s b\frac{S_h}{N_h}S_q - (\omega + \mu_v + \delta_v)S_r, \\
\frac{dI_r}{dt} &= (1-u_1)q\alpha_i b\frac{I_h}{N_h}S_q + \left((1-u_1)p_1\alpha_s b\frac{S_h}{N_h} + (1-u_1)q_1\alpha_i b\frac{I_h}{N_h}\right)I_q \\
&\quad - (\omega + \mu_v + \delta_v)I_r.
\end{aligned} \tag{8.1}$$

with the initial conditions

$S_h(0) = S_{h0}, I_h(0) = I_{h0}, S_q(0) = S_{q0}, I_q(0) = I_{q0}, S_r(0) = S_{r0}, I_r(0) = I_{r0}$.

The study aims to minimize the objective function defined as

$$J(u_1, u_2, u_3) = \int_{t_0}^{t_f} \left(A_1 I_h + A_2 I_q + A_3 I_r + \frac{1}{2}(C_1 u_1^2 + C_2 u_2^2 + C_3 u_3^2) \right) dt. \tag{8.2}$$

where t_f is the final time and $u_1(t), u_2(t), u_3(t) \in [0, 1]$. The coefficients A_1, A_2 and A_3 are weight constants of I_h, I_q and I_r, respectively, while C_1, C_2 and C_3 are the weight constants of personal protection, treatment and use of vaccination, respectively. We consider a quadratic objective functional for the optimal control problem since the cost of implementing a control takes a non linear form (Khan et al., 2019). The aim is to find an optimal control u_1^*, u_2^* and u_3^* such that

$$J(u_1^*, u_2^*, u_3^*) = min(J(u_1, u_2, u_3) : (u_1, u_2, u_3) \in \Omega) \tag{8.3}$$

subject to the system (8.1) where

$$\Omega = \{(u_1, u_2, u_3) : u_i(t) \text{ is Lebesgue measurable and } 0 \leq u_i(t) \leq 1, i = 1, 2, 3\}. \tag{8.4}$$

3.9.1 Existence of the Optimal Control

Theorem 4. *Given the objective functional*

$$J(u_1, u_2, u_3) = \int_{t_0}^{t_f} \left(A_1 I_h + A_2 I_q + A_3 I_r + \frac{1}{2}(C_1 u_1^2 + C_2 u_2^2 + C_3 u_3^2) \right) dt \tag{8.5}$$

subject to the system (8.1) with their initial conditions. Then, there exists an optimal control (u_1^*, u_2^*, u_3^*) and corresponding state solution $S_h^*, I_h^*, S_q^*, I_q^*, S_r^*, I_r^*$ such that $J(u_1^*, u_2^*, u_3^*) = \min_{\Omega}(J(u_1, u_2, u_3)$ if the following conditions are satisfied:

i. The solutions set of system (8.1), with the control functions in (8.4), is non-empty.

ii. The control set Ω is convex and closed.

iii. The right hand side of the state system is bounded by a linear function in the state and control variables.

iv. The integrand of objective functional is convex on Ω.

v. *The integrand of objective functional is bounded by* $\eta_1(|\mu_1|^2 + |\mu_2|^2 + |\mu_3|^2)^{\epsilon/2} - \eta_2$, $\eta_1, \eta_2 > 0$ *and* $\epsilon > 1$.

An existence of the state system with bounded coefficients has been used to give condition (i). The control set is convex and closed by definition hence (ii). The right hand side of the state system satisfies (iii). The state solutions are already bounded hence (iv). For (v) since the state solutions are bounded, then Lipschitz property of the state system with respect to the state variables is satisfied. It can also be seen that there exists positive numbers η_1, η_2 *and a constant* $\epsilon > 1$ *such that,*

$$J(u_1, u_2, u_3) \geq \eta_1(|\mu_1|^2 + |\mu_2|^2 + |\mu_3|^2)^{\epsilon/2} - \eta_2 \tag{8.6}$$

Therefore, the state variables are bounded and the existence of optimal control of the model (8.5) is concluded.

3.9.2 The Hamiltonian and Optimality System

By applying the Pontryagin's Maximum Principle (Pontryagin, 2018), we seek to determine the optimal control $(u_1^*, u_2^*, u_3^*) \in \Omega$ that minimizes the Hamiltonian pointwise subject to the model system (8.1). The associated Hamiltonian is therefore given as:

$$\begin{aligned}
\mathcal{H} = {} & A_1 I_h + A_2 I_q + A_3 I_r + \frac{1}{2}(C_1 u_1^2 + C_2 u_2^2 + C_3 u_3^2) \\
& + \lambda_1 \left((1-u_3)\alpha_h + (u_2 + \gamma_h) I_h - ((1-u_1) b \beta_h \frac{I_q}{N_h} + \mu_h) S_h \right) \\
& + \lambda_2 \left((1-u_1) b \beta_h \frac{I_q}{N_h} S_h - (\mu_h + \delta_h + (u_2 + \gamma_h) I_h \right) \\
& + \lambda_3 \left(\omega S_r - (\mu_v + (1-u_1)\alpha_s b \frac{S_h}{N_h} + (1-u_1)\alpha_i b \frac{I_h}{N_h} + \delta_v) S_q \right) \\
& + \lambda_4 \left(\omega I_r - (\mu_v + (1-u_1)\alpha_s b \frac{S_h}{N_h} + (1-u_1)\alpha_i b \frac{I_h}{N_h} + \delta_v) I_q \right) \\
& + \lambda_5 \left(\alpha_v N_v + (1-u_1) p \alpha_s b \frac{S_h}{N_h} S_q - (\omega + \mu_v + \delta_v) S_r \right) \\
& + \lambda_6 \left((1-u_1) q \alpha_i b \frac{I_h}{N_h} S_q + ((1-u_1) p_1 \alpha_s b \frac{S_h}{N_h} + (1-u_1) q_1 \alpha_i b \frac{I_h}{N_h}) I_q \right) \\
& - \lambda_6 (\omega + \mu_v + \delta_v) I_r),
\end{aligned} \tag{8.7}$$

where $\lambda_1, \lambda_2, \lambda_3, \lambda_4, \lambda_5, \lambda_6$ are the adjoint variables corresponding to state variables $S_h, I_h, S_q, I_q, S_r, I_r$, respectively.

Theorem 5. *Let $S_h, I_h, S_q, I_q, S_r, I_r$ be optimal state solutions with associated optimal control variables u_1, u_2 and u_3 for the optimal control model, there exist co-state variables $\lambda_1, \lambda_2, \lambda_3, \lambda_4, \lambda_5, \lambda_6$ that satisfy,*

$$\frac{d\lambda_1}{dt} = -\frac{\partial \mathcal{H}}{\partial S_h}, \frac{d\lambda_2}{dt} = -\frac{\partial \mathcal{H}}{\partial I_h}, \frac{d\lambda_3}{dt} = -\frac{\partial \mathcal{H}}{\partial S_q}, \frac{d\lambda_4}{dt} = -\frac{\partial \mathcal{H}}{\partial I_q}, \frac{d\lambda_5}{dt} = -\frac{\partial \mathcal{H}}{\partial S_r}, \frac{d\lambda_6}{dt} = -\frac{\partial \mathcal{H}}{\partial I_r}.$$

With transversality conditions

$$\lambda_1(t_f) = \lambda_2(t_f) = \lambda_3(t_f) = \lambda_4(t_f) = \lambda_5(t_f) = \lambda_6(t_f).$$

Moreover, the optimal controls, u_1^*, u_2^* and u_3^* are given by

$$\begin{aligned} u_1^* &= max\left\{0, min\left\{1, \phi\right\}\right\}, \\ u_2^* &= max\left\{0, min\left\{1, \frac{(\lambda_2 - \lambda_1)\gamma_h I_h}{C_2}\right\}\right\}, \\ u_3^* &= max\left\{0, min\left\{1, \frac{(\lambda_2 - \lambda_1) I_h}{C_3}\right\}\right\}. \end{aligned} \tag{8.8}$$

where,

$$\begin{aligned} \phi &= \frac{b\beta_h I_q S_h(\lambda_2 - \lambda_1) + \zeta_1 + \zeta_2}{N_h C_1}. \\ \zeta_1 &= \lambda_s b S_h(pS_q\lambda_5 - S_q\lambda_3 - I_q\lambda_4 + p_1 I_q\lambda_6). \\ \zeta_2 &= \alpha_i b I_h(qS_q\lambda_6 - S_q\lambda_3 - I_q\lambda_4 + q_1 I_q\lambda_6). \end{aligned}$$

Proof. Let (u_1, u_2, u_3) be optimal controls whose existence is assured by Theorem 4. The Pontryagin's Maximum Principle converts the optimal control problem to a static optimization problem that is a problem of minimizing the Hamiltonian $\mathcal{H}$ in the control space. Therefore, to obtain the adjoint system, we take the derivative of the Hamiltonian with respect to state variables, S_h, I_h, S_q, I_q, S_r and I_r, as follows:

$$\frac{d\lambda_1}{dt} = -\frac{\partial \mathcal{H}}{\partial S_h} = -((1-u_1)b\beta_h\frac{I_q}{N_h} + \mu_h)\lambda_1 + (1-u_1)b\beta_h\frac{I_q}{N_h}\lambda_2 - (1-u_1)\alpha_s b$$
$$\frac{S_q}{N_h}\lambda_3 - (1-u_1)\alpha_s b\frac{I_q}{N_h}\lambda_4 + (1-u_1)p\alpha_s b\frac{S_q}{N_h}\lambda_5 + (1-u_1)p_1\alpha_s b\frac{I_q}{N_h}\lambda_6,$$
$$\frac{d\lambda_2}{dt} = -\frac{\partial \mathcal{H}}{\partial I_h} = A_1 + u_2\gamma_h\lambda_1 + \mu_3\lambda_1 - (\mu_h + \delta_h + u_2\gamma_h)\lambda_2 - u_3\lambda_2 - (1-u_1)\alpha_i b\frac{S_q}{N_h}\lambda_3$$
$$- (1-u_1)\alpha_i b\frac{I_q}{N_h}\lambda_4 + (1-u_1)q\alpha_i b\frac{S_q}{N_h}\lambda_6 + (1-u_1)q_1\alpha_i b\frac{I_q}{N_h}\lambda_6,$$
$$\frac{d\lambda_3}{dt} = -\frac{\partial \mathcal{H}}{\partial S_q} = -(\mu_v + (1-u_1)\alpha_s b\frac{S_h}{N_h} + (1-u_1)\alpha_i b\frac{I_h}{N_h} + \delta_v)\lambda_3$$
$$+ (1-u_1)p\alpha_s b\frac{S_h}{N_h}\lambda_5 + (1-u_1)q\alpha_i b\frac{I_h}{N_h}\lambda_6,$$

$$\begin{aligned}
\frac{d\lambda_4}{dt} &= -\frac{\partial \mathcal{H}}{\partial I_q} = A_2 - (1-u_1)b\beta_h\frac{S_h}{N_h}\lambda_1 + (1-u_1)b\beta_h\frac{S_h}{N_h}\lambda_2 \\
&\quad - (\mu_v + (1-u_1)\alpha_s b\frac{S_h}{N_h} + (1-u_1)\alpha_i b\frac{I_h}{N_h} + \delta_v)\lambda_4 \\
&\quad + ((1-u_1)p_1\alpha_s b\frac{S_h}{N_h} + (1-u_1)q_1\alpha_i b\frac{I_h}{N_h})\lambda_6, \qquad (8.9)\\
\frac{d\lambda_5}{dt} &= -\frac{\partial \mathcal{H}}{\partial S_r} = \omega\lambda_3 - (\omega + \mu_v + \delta_v)\lambda_5, \\
\frac{d\lambda_6}{dt} &= -\frac{\partial \mathcal{H}}{\partial I_r} = A_3 + \omega\lambda_4 - (\omega + \mu_v + \delta_v)\lambda_6.
\end{aligned}$$

The characterization of optimal controls u_1, u_2 and u_3 shows that,

$$\frac{\partial \mathcal{H}}{\partial u_1} = \frac{\partial \mathcal{H}}{\partial u_2} = \frac{\partial \mathcal{H}}{\partial u_3} = 0. \qquad (8.10)$$

Thus the optimal solution subject to the constraints $0 \leq u_1 \leq 1$,$0 \leq u_2 \leq 1$, $0 \leq u_3 \leq 1$ is,

$$\begin{aligned}
\mu_1^* &= \frac{b\beta_h I_q S_h(\lambda_2 - \lambda_1) + \zeta_1 + \zeta_2}{N_h C_1}, \\
\mu_2^* &= \frac{(\lambda_2 - \lambda_1)\gamma_h I_h}{C_2}, \qquad (8.11)\\
\mu_3^* &= \frac{(\lambda_2 - \lambda_1)I_h}{C_3}.
\end{aligned}$$

Using equation (8.10), and the lower and upper bounds of the three control measures,

the characterization of optimal controls were obtained as follows;

$$\mu_1^* = \begin{cases} 0, & \text{if } \psi_1 < 0, \\ \psi_1, & \text{if } 0 \leq \psi_1 \leq 1, \\ 1, & \text{if } \psi_1 > 1. \end{cases}$$

$$\mu_2^* = \begin{cases} 0, & \text{if } \psi_2 < 0, \\ \psi_2, & \text{if } 0 \leq \psi_2 \leq 1, \\ 1, & \text{if } \psi_2 > 1. \end{cases} \tag{8.12}$$

$$\mu_3^* = \begin{cases} 0, & \text{if } \psi_3 < 0, \\ \psi_3, & \text{if } 0 \leq \psi_3 \leq 1, \\ 1, & \text{if } \psi_3 > 1. \end{cases}$$

where,

$$\psi_1 = \frac{b\beta_h I_q S_h(\lambda_2 - \lambda_1) + \zeta_1 + \zeta_2}{N_h C_1},$$
$$\psi_2 = \frac{(\lambda_2 - \lambda_1)\gamma_h I_h}{C_2},$$
$$\psi_3 = \frac{(\lambda_2 - \lambda_1) I_h}{C_3}.$$

In compact form, the optimal controls can be written as,

$$\begin{aligned} u_1^* &= max\left\{0, min\left\{1, \psi_1\right\}\right\} \\ u_2^* &= max\left\{0, min\left\{1, \psi_2\right\}\right\} \\ u_3^* &= max\left\{0, min\left\{1, \psi_3\right\}\right\}. \end{aligned} \tag{8.13}$$

□

3.10 Spatial Analysis

Spatial analysis was done by first obtaining the global annual average temperature and rainfall raster data for 2023 with approximately 1km spatial resolution from Environmental Research Data (Envidat) database. The raster data were then clipped to Kenya using

Kenya shapefile in R version 4.4.2 (R Core Team, 2024). The clipped raster data were incorporated into the expression of R_0 in Python, generating the spatial distribution of R_0 over Kenya. To investigate the effectiveness of deltamethrin and permethrin insecticides in the control of mosquitoes, raster data showing the spatial distribution of R_0 when either deltamethrin or permethrin insecticides were used were generated. In addition, since the model was being studied under insecticide resistance, spatial distribution of R_0 when no insecticide was used was also obtained. This depicted a scenario where mosquitoes are resistant to insecticides. The generated raster data were then imported to QGIS to create maps and enhance their appearance.

Chapter 4: Results and Discussion

4.1 Introduction

This chapter presents the results of the numerical simulations performed on the model system (1) and a discussion of the findings.

4.2 Numerical Analysis without Climate Variables

Due to the unavailability of freely accessible high-resolution climatic data with good temporal coverage for Kenya, numerical simulations of model system (1) was performed without considering climatic influence. The model system is solved numerically using the package scipy.integrate.odeint in Python language. The dynamics of each state variable of our model is illustrated using constant parameter values presented in Table 4.1 with the following initial conditions: $S_h = 7000$, $I_h = 300$, $S_q = 300$, $I_q = 50$, $S_r = 800$, $I_r = 200$ which were obtained by randomly selecting values within biologically meaningful ranges. The plots showing the dynamics of the human and mosquito population with time in the presence of insecticide resistance are shown in Figure 4.1.

In Figure 4.1 (a-b), the population of susceptible humans initially declines as the population of infected humans rise due to the interaction of infected questing mosquitoes with susceptible humans. Since mosquitoes are sensitive to insecticides, their population declines as some die due to use of insecticides especially in the first 10 days. Therefore, the population of infected humans continually declines as the number of mosquitoes reduces and levels off at the disease free equilibrium E_0 (Figure 4.1 (b)). Due to the high resting rate of questing mosquitoes and death rate due to use of insecticides, the infected questing population declines to zero with the susceptible questing mosquitoes stabilizing at the disease free equilibrium E_0 (Figure 4.1 (c-d)). Consequently, the population of susceptible resting mosquitoes increases slightly as more susceptible questing mosquitoes move to this compartment (Figure 4.1 (e)).

When $\delta_v = 0$, that is mosquitoes are resistant to insecticides, the disease free equilibrium of the system becomes unstable as $R_0 > 1$. The population of susceptible humans declines as some of them get infected through bites from infected mosquitoes (Figure 4.2 (a)). This leads to an increase in the number of infected humans (Figure 4.2 (b)). On the other hand, the population of susceptible resting mosquitoes initially increases as

more mosquitoes are recruited through birth (Figure 4.2 (e)). Before mosquitoes lay their eggs, they require blood for their eggs to be fertilized therefore, the resting population move to the questing population to interact with the human population and obtain a blood meal. This explains the similar increase in the population of susceptible questing population. Additionally, between day 0 to about 16 days, the population of susceptible mosquitoes increases steadily and afterwards declines. In comparison, between day 0 and day 5, the infected mosquito population decreases, likely due to unsuccessful blood-feeding attempts, as susceptible mosquitoes outnumber infected ones during this period. Afterwards, the population of infected mosquitoes begins to grow from day 5 coinciding with the asexual replication experienced by malaria parasites every 5-16 days releasing merozoites into the blood cell which attack the red blood cells. Inside the red blood cells the parasite progresses with its growth stages infecting more vulnerable red blood cells. As there is no induced mosquito death rate due to the use of insecticides, the population of infected mosquitoes continually grows resulting to more infected human population, therefore malaria disease persists in the population, $R_0 = 1.2721 > 1$.

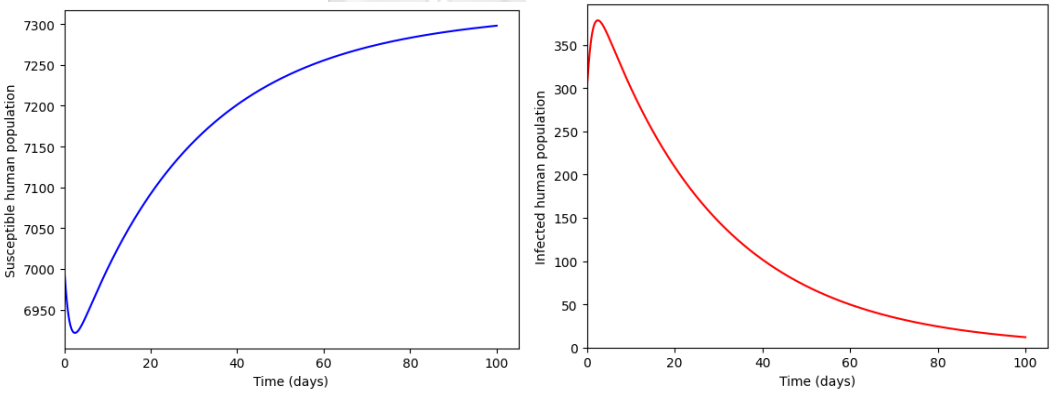

(a) Susceptible humans

(b) Infected humans

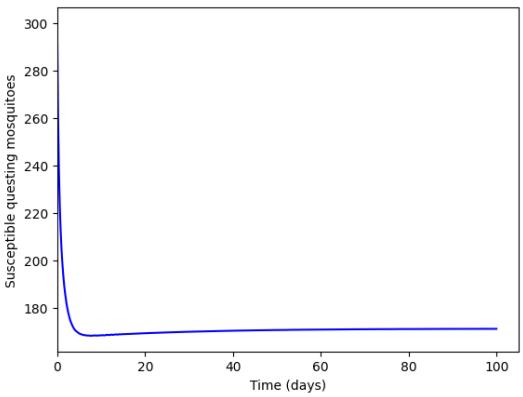

(c) Susceptible questing

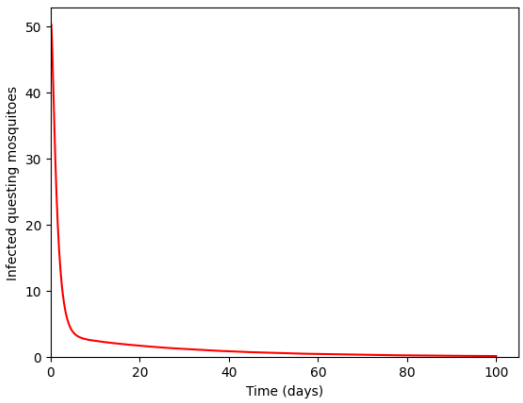

(d) Infected questing

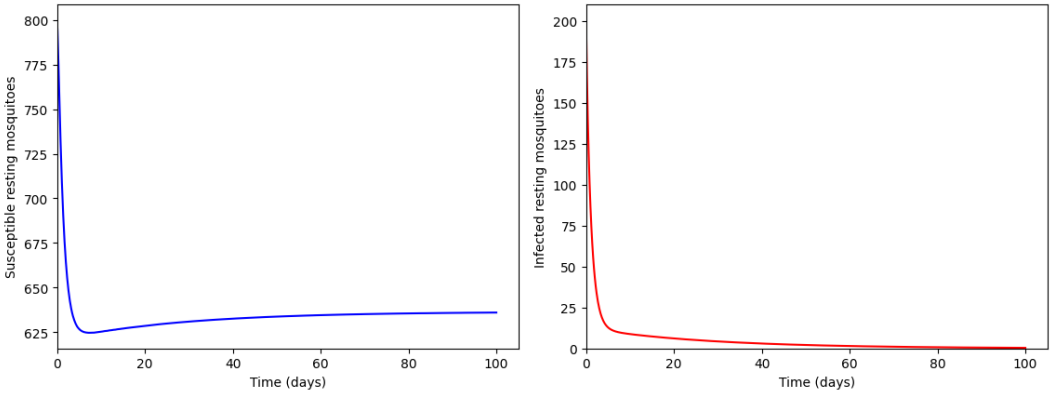

(e) Susceptible resting (f) Infected resting

Figure 4.1: Graphs showing the dynamics of human and mosquito population when mosquitoes are sensitive to insecticides, $\delta_v = 0.4862$, $R_0 = 0.4821 < 1$.

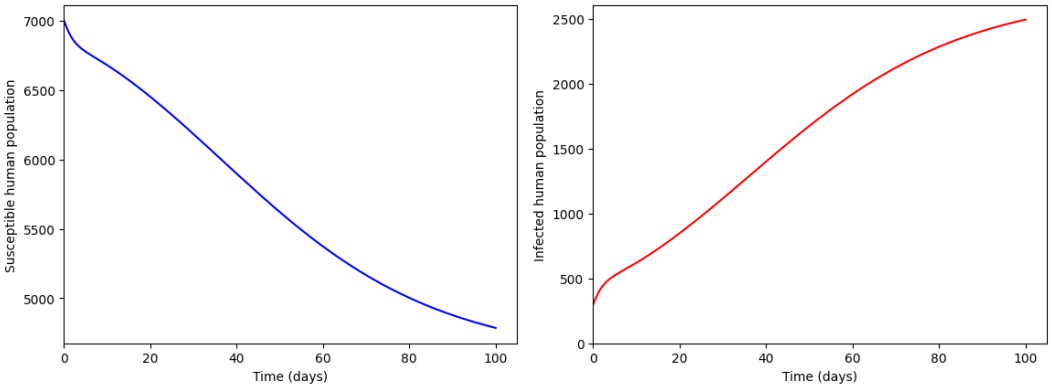

(a) Susceptible humans (b) Infected humans

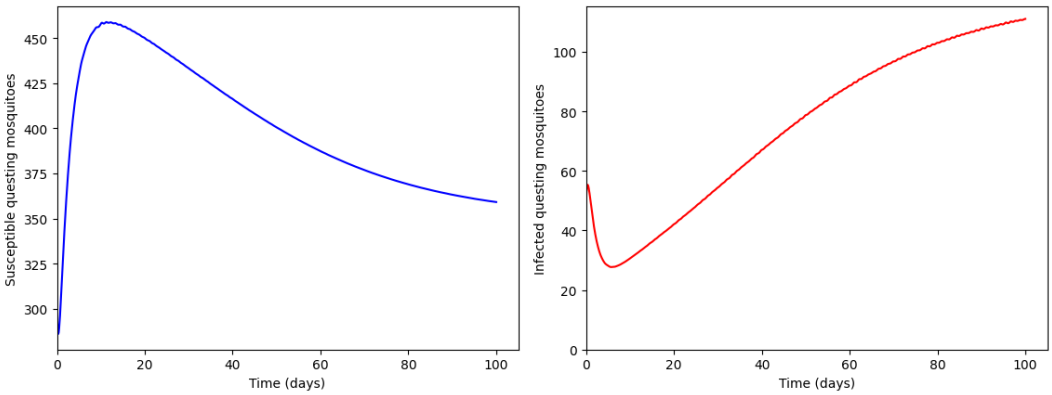

(c) Susceptible questing (d) Infected questing

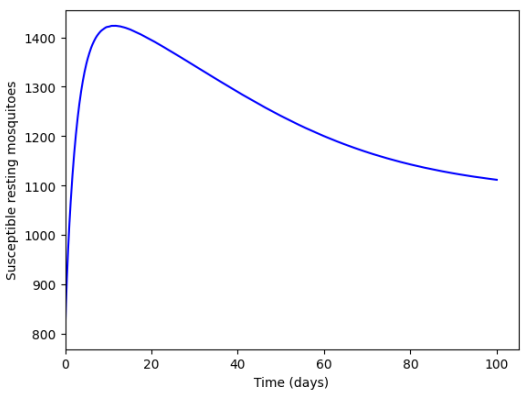

(e) Susceptible resting

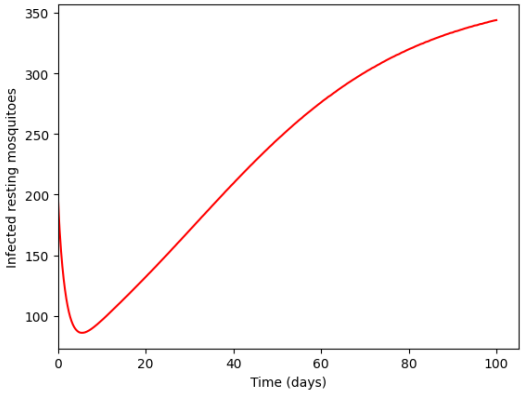

(f) Infected resting

Figure 4.2: Graphs showing the dynamics of human and mosquito population when mosquitoes are resistant to insecticides, $\delta_v = 0$, $R_0 = 1.2721 > 1$.

4.3 Spatial Distribution of Malaria Basic Reproduction Number over Kenya

Using the expression of the basic reproduction number for our model system (1) with temperature and rainfall raster data, a spatial distribution of R_0 was obtained.

Annual average temperature and rainfall raster data for 2023 with approximately 1km spatial resolution was obtained from Envidat database (Karger et al., 2019). We incorporated the temperature and rainfall dependent parameters into the expression of the basic reproduction number and investigated the effectiveness of deltamethrin and permethrin insecticides in the control of mosquitoes. Figure 4.3 (a) and Figure 4.4 (a) shows the spatial distribution of R_0 when deltamethrin was used to induced mosquito mortality rate, $\delta_v = 0.4862$, and when permethrin was used to induced mosquito mortality rate, $\delta_v = 0.2562$, respectively. It is evident from the two figures that with a higher induced mosquito mortality rate, the values of R_0 were lower, ranging between 0 to 0.3 for $\delta_v = 0.4862$. With the use of permethrin, the maximum value of R_0 over Kenya ranged between 0.3 to 0.6. When no insecticide was used to control the population of malaria vectors, the values of R_0 over Kenya increased with the maximum value ranging between 0.9 to 1.2. In Figure 4.3 (b) and Figure 4.4 (b), the eastern region and some parts of the western region of Kenya experienced high malaria transmission which could be attributed to the good climatic conditions favouring the survival of malaria vectors in these regions. It has been highlighted in Kenya (2020) that favourable climatic conditions enhances the breeding of malaria vectors increasing the transmission intensity of the disease. Within the central and rift valley regions of Kenya, the value of R_0 was lower and could have

been due to the low temperatures and high rainfall not favouring development rate of malaria vectors (Figure 4.3 (b) and Figure 4.4 (b)).

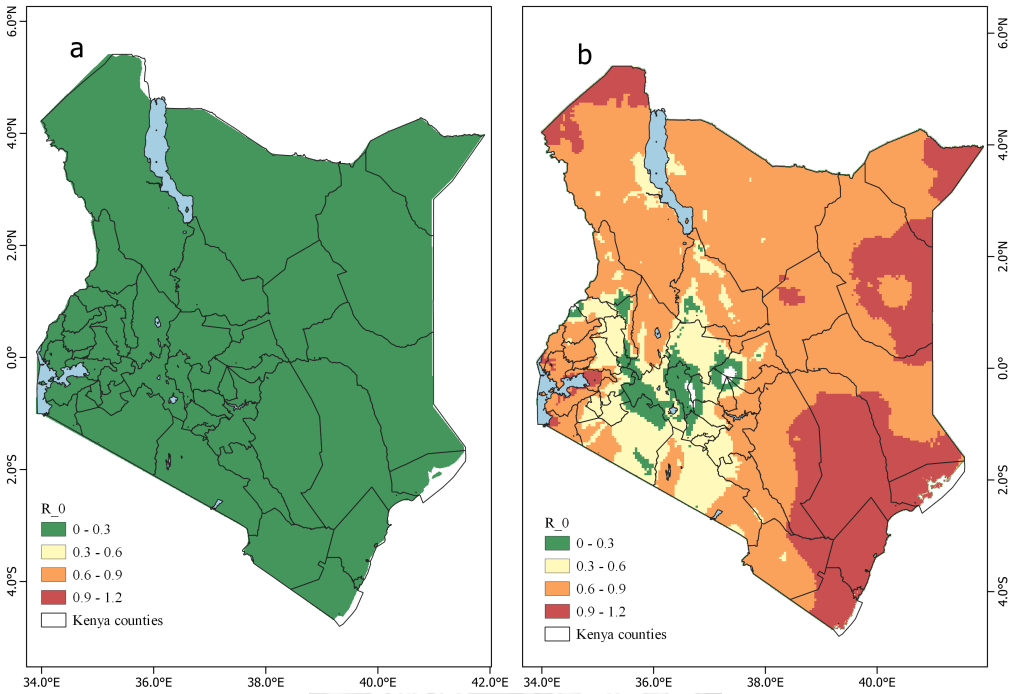

Figure 4.3: Simulation of basic reproduction number with temperature and rainfall dependent parameters when (a) deltamethrin insecticide is used, $\delta_v = 0.4862$ and (b) no insecticide is used, $\delta_v = 0$.

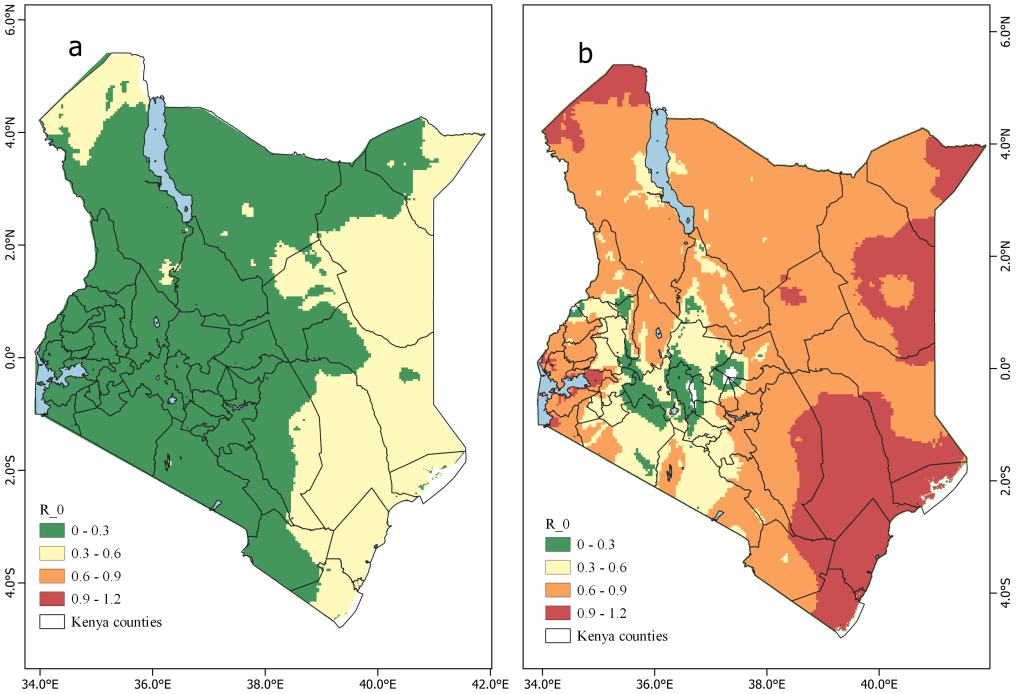

Figure 4.4: Simulation of basic reproduction number with temperature and rainfall dependent parameters when (a) permethrin insecticide is used, $\delta_v = 0.2562$ and (b) no insecticide is used, $\delta_v = 0$.

4.4 Sensitivity Analysis

Sensitivity analysis was carried out to determine the model's robustness to parameter values and identify variables that significantly influence the spread of the disease under study.

4.4.1 Local Sensitivity Analysis

To identify parameters that significantly affect R_0 and should be targeted in control interventions, the forward sensitivity index which uses the normalized forward sensitivity index of a variable to a parameter was utilized.

Definition: The normalized forward sensitivity index of R_0 that depends differentiably on a parameter η is defined as

$$S_{\eta}^{R_0} = \frac{\partial R_0}{\partial \eta} \frac{\eta}{R_0}. \tag{9}$$

Using the formulation in (9) and the parameter values in Table 4.1, the local sensitivity indices (SI) of R_0 relative to the model parameters was calculated using Mathematica software and the results shown in Table 4.2.

Table 4.1: Parameters of the malaria model 1

Parameter	**Description**	**Value**	**Source**
α_h	Human recruitment rate	0.4559 day $^{-1}$	Group (2021), Ngonghala (2022)
b	Mosquito biting rate	5 day $^{-1}$	Assumed
β_h	Transition probability of susceptible humans to infectious humans	0.5	Assumed
γ_h	Recovery rate amongst humans	0.05	Assumed
μ_h	Natural human mortality rate	0.00004559	Agency (2009), Ngonghala et al. (2012)
δ_h	Malaria induced human mortality rate	0.0002	Chitnis et al. (2008a), Ngonghala et al. (2012)
α_v	Mosquito birth rate	0.6	Assumed

Continued on next page

Table 4.1 – *Continued from previous page*

Parameter	Description	Value	Source
μ_v	Natural mosquito mortality rate	0.05	Ngonghala et al. (2012), Tchoumi et al. (2018)
ω	Rate at which resting vectors are attracted to humans at the human habitat	0.8	Assumed
p	Probability that a type S_q vector successfully takes a blood meal from a susceptible human	0.6	Assumed
q	Probability that a type S_q vector successfully takes a blood meal from an infectious human	0.5	Assumed
ϵ	Efficacy of insecticides	0.7	Montoya and Romero-Leiton (2020)
κ	Death rate of mosquitoes due to insecticides	0.7311	Estimated
ρ	Resistant acquisition ratio to insecticides	0.05	Montoya and Romero-Leiton (2020)
α_s	Resting rate of susceptible mosquitoes	0.6666	Tchoumi et al. (2018)
α_i	Resting rate of infected mosquitoes	0.6666	Tchoumi et al. (2018)
p_1	Probability that a type I_q vector successfully takes a blood meal from a susceptible human	0.5	Assumed
q_1	Probability that a type I_q vector successfully takes a blood meal from an infectious human	0.6	Assumed
T_1	Mean temperature in the absence of seasonality	19.9℃	Parham and Michael (2010)
B_E	Number of eggs laid per adult per oviposition	200	Parham and Michael (2010)

Continued on next page

Table 4.1 – *Continued from previous page*

Parameter	Description	Value	Source
Γ_E	Daily survival probabilities of eggs	0.9	Parham and Michael (2010)
Γ_L	Daily survival probabilities of larvae	0.25	Parham and Michael (2010)
Γ_P	Daily survival probabilities of pupae	0.75	Parham and Michael (2010)
R_L	Rainfall limit beyond which breeding sites get flushed out and no immature stages survive	250mm	Assumed

Table 4.2: Sensitivity indices of R_0 with respect to the parameters

Parameter	Sensitivity index
α_s	-0.808491
δ_v	-0.674513
ω	+0.550067
q	+0.5
α_v	+0.5
α_i	+0.5
β_h	+0.5
N_v	+0.5
γ_h	-0.498252
α_h	-0.308491
μ_h	+0.308166
p	+0.218713
b	+0.191509
N_h	-0.191509
p_1	+0.127254
μ_v	-0.0670624
δ_h	-0.00142358

The sensitivity indices in Table 4.2 illustrates how changes in parameters translate into variations in R_0. R_0 is most sensitive to the resting rate of susceptible mosquitoes with a sensitivity index of -0.808491. Hence a 100% increase (or decrease) in α_s leads to a 80.85% decrease (or increase) in R_0. Therefore, leading to a reduction in malaria infection. Increasing induced mosquito death rate also has a negative influence on the progression of malaria disease as 100% increase (or decrease) in δ_v leads to a 67.45% decrease (or increase) on R_0.

On the other hand, the rate at which resting vectors are attracted to humans at the human habitat has a positive influence on disease transmission, as 100% increase (or decrease) in ω would increase (or decrease) the threshold parameter R_0 by 55.01%. Similarly, the parameters q, α_v, α_i, β_h and N_v increase (or decrease) R_0 when they are increased (or decreased). Epidemiologically, increasing mosquito birth rate α_v, would increase the population of mosquitoes making more humans susceptible to mosquito bites. Additionally, higher transition probability of susceptible humans to infectious humans β_h increase the severity of malaria infection. Hence, a 100% increase (or decrease) in α_v and β_h increases (or decreases) R_0 by 50%.

Any interventions that reduces the population of mosquitoes and the number of infected individuals will certainly result in the reduction of R_0. Therefore, an increase in the death rate of mosquitoes will eventually lead to a significant reduction in R_0. This can be achieved by increasing the use of insecticides especially those which the mosquitoes have low resistance towards. Additionally, increasing the recovery rate of infected humans through the use of antimalarial treatment such as use of artemisinin based combination therapy (ACT) will reduce the basic reproduction number R_0.

To further investigate the parameter influence on disease progression, we generated the partial rank correlation coefficients(PRCCs) for each parameter in the expression of R_0. The results are displayed in the next section.

4.4.2 Global Sensitivity Analysis

Global sensitivity analysis (GSA) examines how an epidemic model responds to parameter variations within a larger range (Wu et al., 2013). Using the approach described in Wu et al. (2013), the PRCCs of the basic reproduction number R_0 and each of the parameters in Table 3.2 were derived. Using 500 simulations per run of the Latin Hypercube Sampling

(LHS) scheme (Stein, 1987), the established PRCCs were derived and presented in Figure 4.5.

In comparison to the results presented in Table 4.2, the parameter with the highest influence on R_0 according to the PRCCs is the mosquito mortality rate due to the use of insecticides δ_v (Figure 4.5). This is closely followed by the resting rate of susceptible mosquitoes α_s, which has a negative influence on R_0 and the parameter corresponding to the probability of type S_q vector successfully taking a blood meal from an infectious human q, which has a positive influence on R_0.

Similar to the results presented in Table 4.2, an increase (or decrease) in α_h, μ_v, δ_h, γ_h and N_h leads to a decrease (or increase) in R_0 as the parameters have negative influence on R_0. However, unlike Table 4.2, there is an increase in the influence of parameters α_h, μ_v and γ_h in Figure 4.5. Likewise, there is a increase in the positive influence of the parameters p_1, p, b, α_v, ω, α_i, μ_h, β_h and N_v on R_0 in PRCCs results (Figure 4.5) compared to the results in Table 4.2.

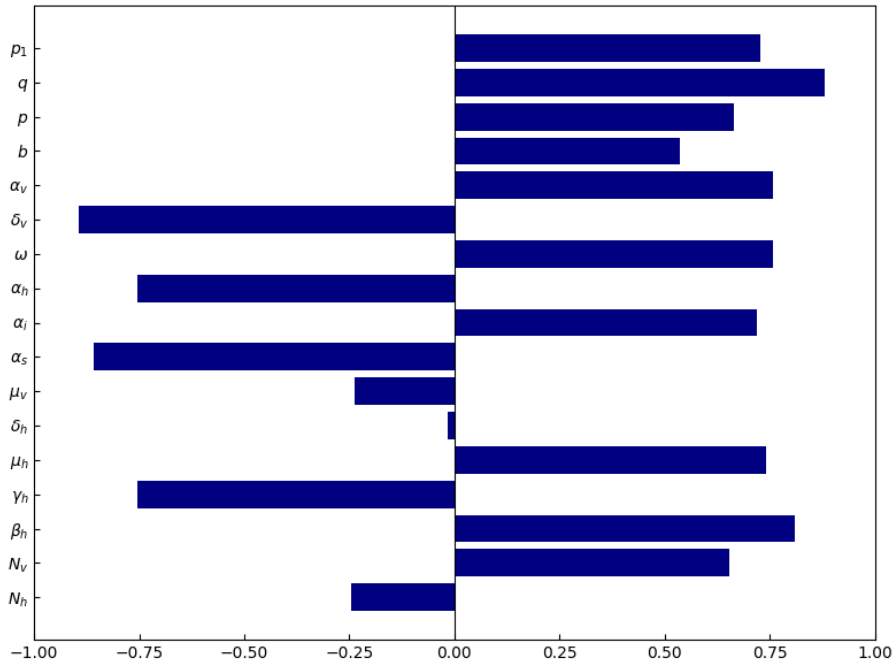

Figure 4.5: Tornado plot of partial rank correlation coefficients (PRCCs) of parameters influencing R_0. Parameters with $PRCC > 0$ increase the value of R_0 while those with $PRCC < 0$ decrease the value of R_0.

4.5 Malaria Prevalence in the Absence and Presence of Insecticide Resistance

The impact of insecticide use in malaria transmission was investigated by considering two pyrethroid insecticides, deltamethrin and permethrin insecticides. The results in Figure 4.6 reveals that malaria prevalence is lower when deltamethrin is used compared to when permethrin is used, with an area under curve (AUC) difference of 52.51%.days. The smaller AUC difference between the two insecticides curves indicate that they have similar efficacy in mosquito control. However, since the curve for deltamethrin declines faster to zero compared to permethrin curve, deltamethrin should be considered to achieve lower malaria prevalence faster. The reduction in malaria prevalence when deltamethrin or permethrin insecticide is used implies that a proportion of mosquitoes are sensitive to insecticides hence, mosquito population reduces with time, lowering malaria transmission rate.

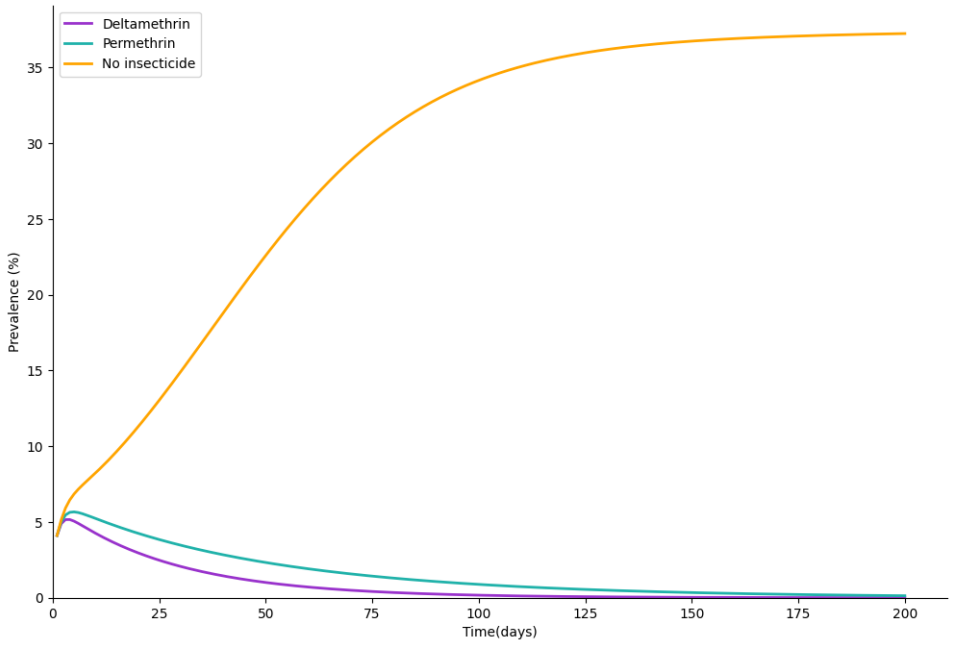

Figure 4.6: A graph showing malaria prevalence when mosquitoes are sensitive to deltamethrin or permethrin insecticides use, and when mosquitoes are resistant to insecticides.

In comparison, when no insecticide is used, depicting a scenario where mosquitoes are resistant to insecticides, malaria prevalence increases and stabilizes after 150 days% (Figure 4.6). The AUC difference between use of deltamethrin and no use of insecticide, and between use of permethrin and no use of insecticide was 780.38%.days and 727.88%.days,

respectively. The larger AUC difference (780.38%.days and 727.88%.days) implies that when mosquitoes are resistant to insecticides, the prevalence of malaria will rapidly grow within a population and stabilize after sometime. However, when a proportion of mosquitoes are sensitive to insecticides, the spread of malaria can be contained within a population.

4.6 Numerical Simulation of Optimal Control Problem

To illustrate the viability of the theoretical results and control strategies obtained in the formulation of optimal control problem, numerical simulation were performed in Python language. The simulation were performed to investigate the effectiveness of personal protection, treatment and vaccination as control strategies to curb the spread of malaria. This was done by considering four scenarios as follows:

4.6.1 Personal Protection $u_1 \neq 0$, Treatment $u_2 \neq 0$, and Vaccination $u_3 = 0$

Figure 4.7 depicts a scenario where only personal protection and treatment are implemented to control malaria transmission. The simulation graph in Figure 4.7 (a) shows that when the two control interventions are implemented, the number of infected humans decreases steadily and levels off to zero after 10 days. When no control intervention is implemented, there is an increase in the number of infected humans with a peak at day 8 and afterwards a steady decline. The decline could be attributed to the reduction in the number of infected mosquitoes as shown in Figure 4.7 (b) and Figure 4.7 (c).

In Figure 4.7 (b), there is an increase in the number of infected questing mosquitoes between day 0 and 5 as infected resting mosquitoes move to this compartment in search of a blood meal. Additionally, the higher number of infected questing mosquitoes when interventions are used, compared to when no intervention is used, may be attributed to the development of insecticide resistance, which can prolong mosquito lifespan. This is however dependent on the resistant intensity. For instance, in Figure 4.7 (b) the infected questing mosquitoes may be having a lower resistance intensity which could explain the steady decline in their population before day 10 when interventions are used. Similar to Figure 4.7 (a), the simulation curves in Figure 4.7 (b) and Figure 4.7 (c) levels off to zero after 10 days when the two control strategies are implemented. On the other hand, without interventions, the population of infected mosquitoes decreases gradually due to

natural death and stabilizes after 40 days.

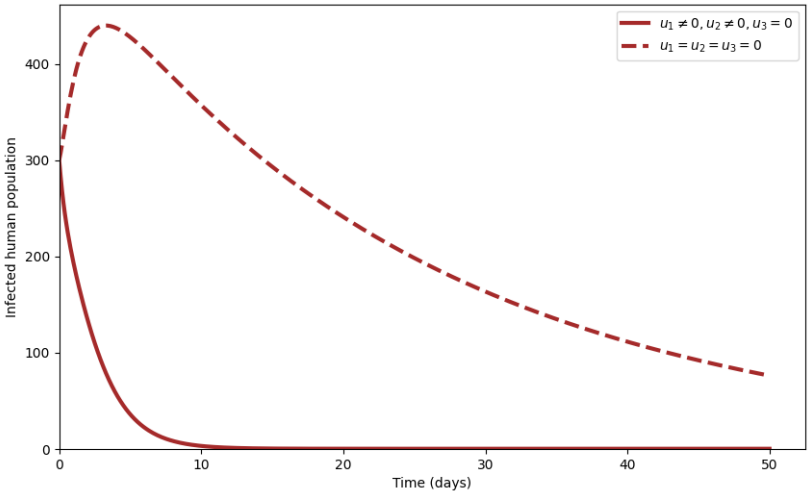

(a) Infected humans

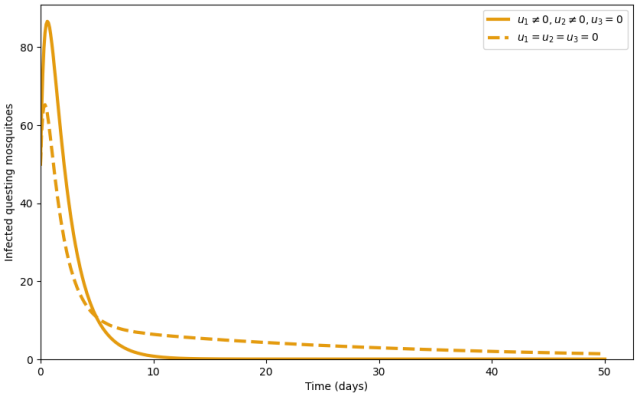

(b) Infected questing mosquitoes

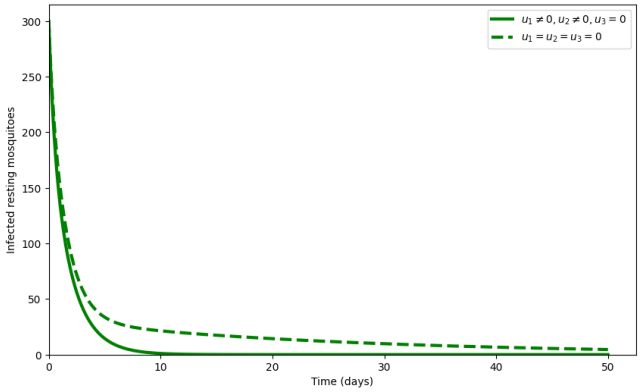

(c) Infected resting mosquitoes

Figure 4.7: Graph showing the effect of implementing personal protection u_1 and treatment u_2 control measures on infected human and mosquito population.

4.6.2 Personal Protection $u_1 \neq 0$, Treatment $u_2 = 0$, and Vaccination $u_3 \neq 0$

In this scenario, personal protection and vaccination were implemented to control the spread of malaria. The population of infected humans initially increases with a peak at day 5 in both cases where control interventions are implemented and when no control intervention is implemented (Figure 4.8 (a)). After 5 days, the two simulation curves in Figure 4.8 (a) gain a gradual decrease overtime. However, the number of infected humans when control interventions is used is lower compared to when no control interventions is used.

Other than infected resting mosquitoes moving to the infected questing population, the

increase in the questing population could also be due to the development of insecticide resistance against insecticide based control interventions such as LLINs. This could explain why the population of infected questing mosquitoes is higher when the two interventions are used compared to when no control intervention is used (Figure 4.8 (b)). Due to a lower resistant intensity, the population of infected questing mosquitoes gradually declines as more mosquitoes die due to exposure to insecticides when interventions are used. Eventually, the population of infected mosquitoes stabilizes after 40 days (Figure 4.8 (b), Figure 4.8 (c)).

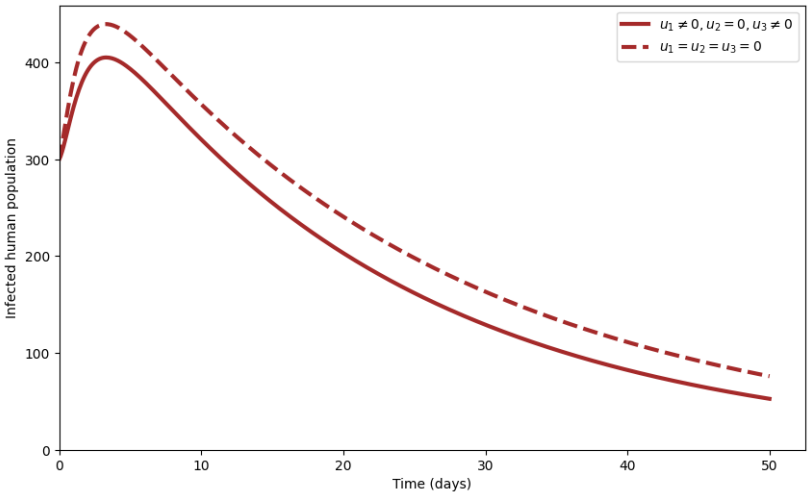

(d) Infected humans

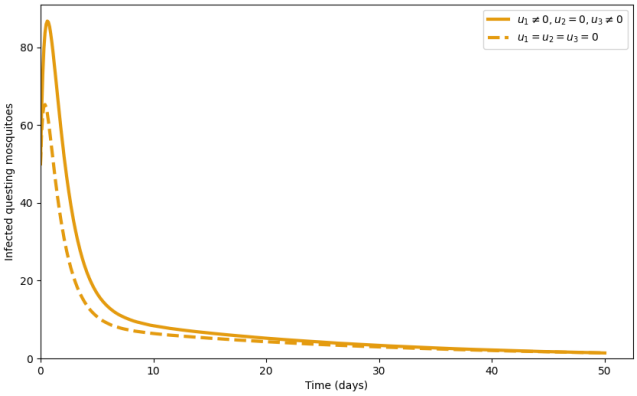

(e) Infected questing mosquitoes

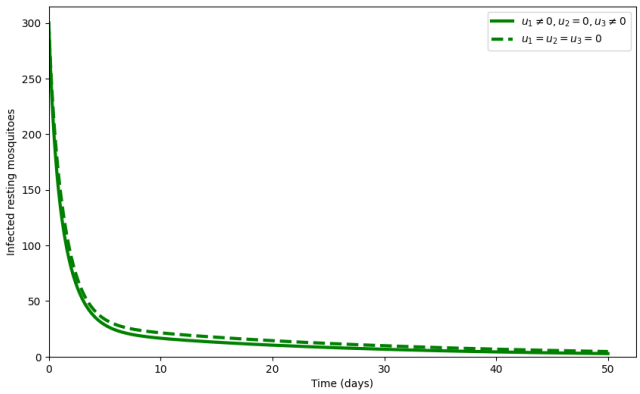

(f) Infected resting mosquitoes

Figure 4.8: Graph showing the effect of implementing personal protection u_1 and vaccination u_3 control measures on infected human and mosquito population.

4.6.3 Personal Protection $u_1 = 0$, Treatment $u_2 \neq 0$, and Vaccination $u_3 \neq 0$

Similar to the results obtained in Figure 4.7 (a), when treatment and vaccination are used as control interventions against malaria spread, the number of infected humans decreases

steadily and levels off to zero after 10 days (Figure 4.9 (a)). When no control intervention is implemented, there is an increase in the number of infected humans with a peak at day 8 and afterwards a steady decline (Figure 4.9 (a)).

In Figure 4.9 (b) and Figure 4.9 (c), similar dynamics is shown within the first 5 days when control intervention is used and when no control intervention is utilized. Afterwards, the population of infected mosquitoes reduces and levels off to zero when the two interventions are implemented. With no control interventions, a gradual decline in the population of infected mosquitoes is experienced and stabilizes at about 40 days (Figure 4.9 (b), Figure 4.9 (c)).

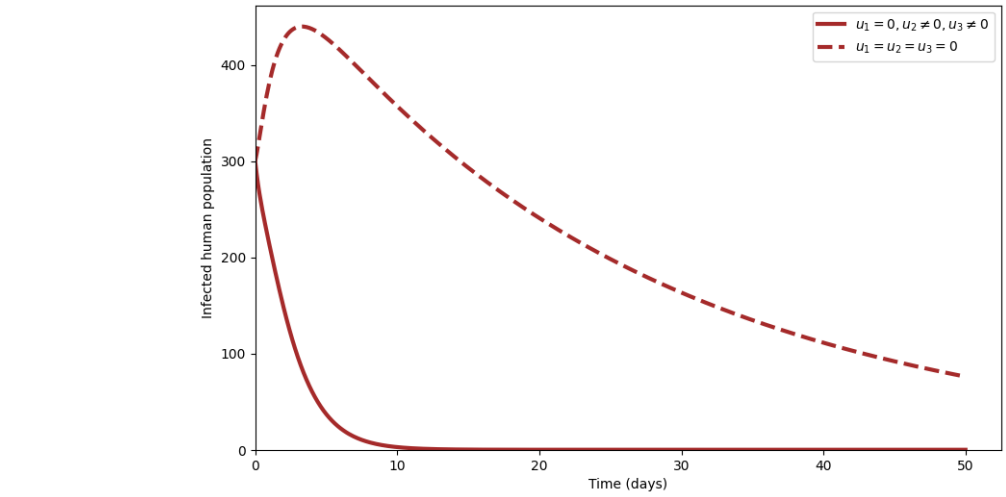

(a) Infected humans

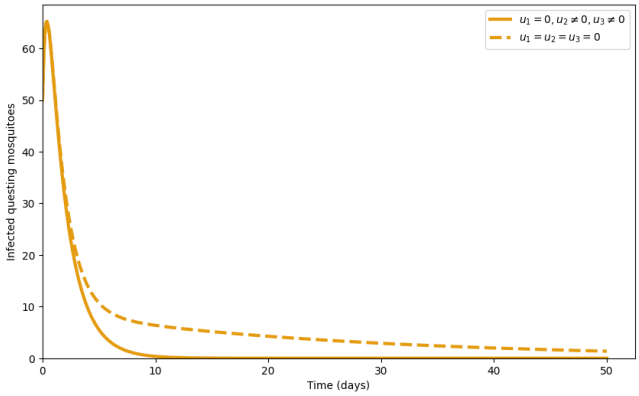

(b) Infected questing mosquitoes

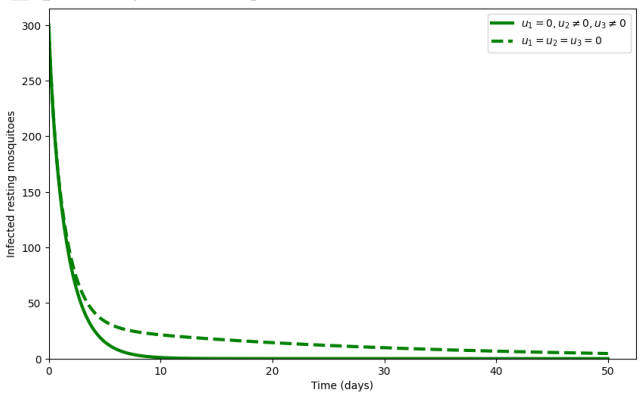

(c) Infected resting mosquitoes

Figure 4.9: Graph showing the effect of implementing treatment u_2 and vaccination u_3 control measures on infected human and mosquito population.

4.6.4 Personal Protection $u_1 \neq 0$, Treatment $u_2 \neq 0$, and Vaccination $u_3 \neq 0$

Figure 4.10 depicts a scenario where three control measures that is, personal protection u_1, treatment u_2, and vaccination u_3 are implemented in the control of malaria. Similar dynamics depicted in Figure 4.7 (a) and Figure 4.9 (a) are shown in Figure 4.10 (a). Unlike Figure 4.8 (a), where only personal protection and vaccination were implemented, utilizing all controls reduces the number of infected humans leveling off to zero after 10 days. This also shows that treatment is more effective in controlling malaria transmission compared to the use of personal protection or vaccination only (Figure A.1 (a), Figure A.2 (a), Figure A.3 (a)). However, due to the potential drug resistance that could emerge with the persistent use of antimalarial treatment, there is need to simultaneously utilize the three control measures to help mitigate the spread of malaria disease. Additionally, the supply of malaria vaccine could be increased to assess its impact in malaria transmission. Similar dynamics of infected mosquitoes depicted in Figure 4.7 (b) and Figure 4.7 (c) are also shown in Figure 4.10 (b) and Figure 4.10 (c). There is an increase in the population of infected questing mosquitoes between day 0 and day 5. With the implementation of controls, the population of infected mosquitoes levels off to zero after 10 days. However, with no controls implemented, a gradual decrease in the population of infected mosquitoes is experienced which stabilizes after 40 days.

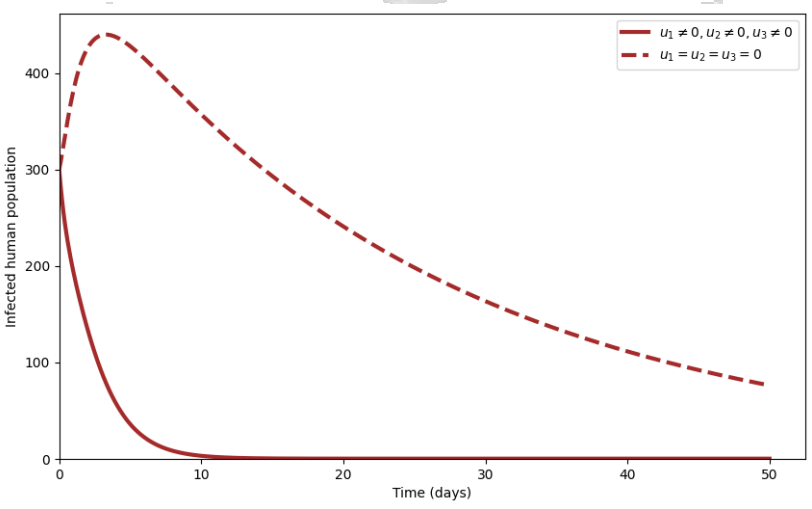

(a) Infected humans

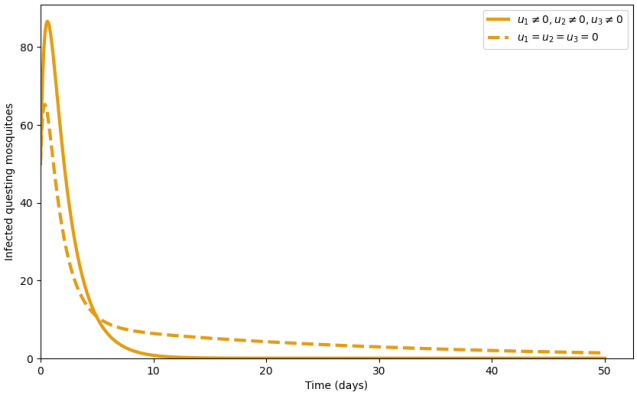

(b) Infected questing mosquitoes

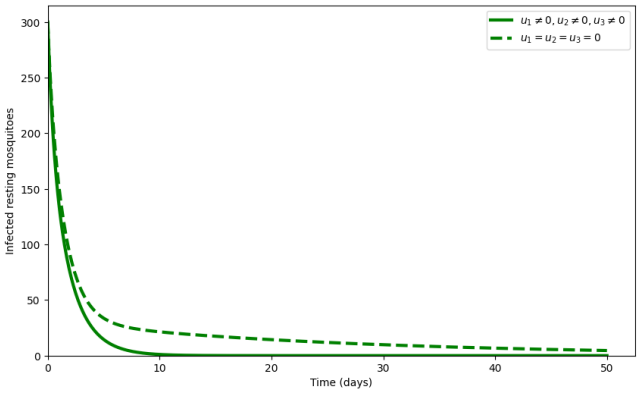

(c) Infected resting mosquitoes

Figure 4.10: Graph showing the effect of implementing personal protection u_1, treatment u_2, and vaccination u_3 control measures on infected human and mosquito population.

Chapter 5: Conclusion and Recommendations

Our analysis suggests that in order to understand the dynamics of indirectly transmitted disease such as malaria, where the transmitting vector inhabits different environments than humans and adopts to different habitats, incorporating the vector's behaviour and climatic dependent parameters is necessary in the development of mathematical models. The slight increase in the population of susceptible resting mosquitoes as the susceptible questing mosquitoes returned to the breeding sites revealed that mosquito behaviour influence the dynamics of malaria disease.

Additionally, the impact of insecticide resistance and climatic variation in malaria transmission has also been investigated in our analysis. In the presence of insecticide resistance, the reproduction number was greater than one which implied that the disease persisted in the population. The spatial distribution of the reproduction number across Kenya further showed that regions whose climatic conditions were favourable for malaria vector survival experienced higher malaria transmission compared to areas whose climatic conditions were less favourable for vector survival and development.

Amidst the changing climatic conditions, when mosquitoes are sensitive to insecticides, malaria transmission can still be contained. However, due to the continuous exposure of these insecticides to mosquitoes especially in the use of insecticide treated nets or larvicides, mosquitoes will ultimately develop resistance to these insecticides. Additionally, climate change also creates suitable habitats for malaria vectors by creating more breeding sites or providing favourable conditions for the survival of these vectors. This will eventually make more areas endemic to malaria disease. Hence, ways to control the spread of malaria amidst insecticide resistance and climatic variation should still be explored. Interventions could be targeted to mosquito breeding sites in order to reduce the population of vectors that emerge and develop into adults.

In order to determine the optimal combination strategies for malaria control in Kenya, three control interventions that is personal protection, treatment and vaccination were considered. The best control was when the three interventions were used simultaneously. Although considering two interventions that is treatment and personal protections or treatment and vaccination had the same dynamics as using the three interventions, relying solely on either of the two approach is not advisable due to the risk of drug resistance

arising from the continuous use of antimalarial treatment. Therefore, alternative strategies, such as increasing the supply of malaria vaccines, should be explored to assess their potential impact in controlling the spread of malaria. Overall the number of infected individuals declined after 10 days with the implementation of all three controls. In contrast, without any control measures, it took up to 40 days for the infected population to decrease. This shows that implementation of personal protection, treatment and vaccination to control malaria spread have an impact in reducing malaria transmission and therefore should be implemented by national malaria control program stakeholders in the fight against malaria in Kenya.

This study tried to capture the existing dynamical changes in malaria transmission by incorporating mosquito behaviour and climatic variation. However, it did not consider human related activities, such as the use of agricultural pesticides on farms, which contribute to insecticide resistance as mosquitoes are exposed to these chemicals while seeking for a blood meal. Further improvements could be done on the model by incorporating human related activities and studying its impact in malaria transmission. The study also considered only the adult mosquito population and two states of the human population in the analysis. Improvements could be done to the existing model by adding a compartment of the juvenile mosquitoes and the population of recovered humans to assess their implications in malaria transmission. Additionally, while obtaining the spatial distribution of the reproduction number, we chose raster data with a finer spatial resolution forfeiting the temporal aspect. This decision was driven by the fact that freely available weather data involve a tradeoff between spatial resolution and temporal coverage. With sufficient resources to acquire high resolution spatial weather data with good temporal coverage, monthly malaria transmission patterns could be mapped to effectively monitor the spread of malaria in Kenya.

While this study highlighted the effectiveness of deltamethrin and permethrin insecticides in reducing malaria prevalence, it did not consider their economic impact especially in Kenya. Therefore, future studies could focus on conducting a cost-benefit analysis of these insecticides on malaria control. Such analysis would support the development of more sustainable and economically efficient vector control strategies.

References

Abiodun, G. J., Maharaj, R., Witbooi, P., and Okosun, K. O. (2016). Modelling the influence of temperature and rainfall on the population dynamics of Anopheles arabiensis. *Malaria Journal*, 15(1):364.

Abiodun, G. J., Witbooi, P., and Okosun, K. O. (2018). Modelling the impact of climatic variables on malaria transmission. *Hacettepe Journal of Mathematics and Statistics*, 47(2):219–235.

Agency, C. I. (2009). *The world factbook 2009*. Central Intelligence Agency.

Agyekum, T. P., Botwe, P. K., Arko-Mensah, J., Issah, I., Acquah, A. A., Hogarh, J. N., Dwomoh, D., Robins, T. G., and Fobil, J. N. (2021). A systematic review of the effects of temperature on Anopheles mosquito development and survival: implications for malaria control in a future warmer climate. *International Journal of Environmental Research and Public Health*, 18(14):7255.

Anderson, R. M. and May, R. M. (1991). *Infectious diseases of humans: dynamics and control*. Oxford University Press.

Azu-Tungmah, G. T., Oduro, F. T., and Okyere, G. A. (2019). Analysis of an age-structured malaria model incorporating infants and pregnant women. *Journal of Advances in Mathematics and Computer Science*, 30(4):1–21.

Bailey, N. (1982). *The Biomathematics of Malaria*. London: Charles Griffin & Co Ltd.

Barbosa, S. and Hastings, I. M. (2012). The importance of modelling the spread of insecticide resistance in a heterogeneous environment: the example of adding synergists to bed nets. *Malaria Journal*, 11(258):1–12.

Barnes, K. G., Weedall, G. D., Ndula, M., Irving, H., Mzihalowa, T., Hemingway, J., and Wondji, C. S. (2017). Genomic footprints of selective sweeps from metabolic resistance to pyrethroids in african malaria vectors are driven by scale up of insecticide-based vector control. *PLoS Genetics*, 13(2):e1006539.

Bhatt, S., Weiss, D., Cameron, E., Bisanzio, D., Mappin, B., Dalrymple, U., Battle, K., Moyes, C., Henry, A., Eckhoff, P., et al. (2015). The effect of malaria control on plasmodium falciparum in Africa between 2000 and 2015. *Nature*, 526(7572):207–211.

Bhattacharya, S., Sharma, C., Dhiman, R., and Mitra, A. (2006). Climate change and malaria in India. *Current Science*, 90(3):369–375.

Bisanzio, D., Ally, M., Ali, A. S., Kitojo, C., Serbantez, N., Kisinza, W. N., Magesa, S., and Reithinger, R. (2022). Modelling insecticide resistance of malaria vector populations in Tanzania. *The American Journal of Tropical Medicine and Hygiene*, 107(2):308.

Cai, L., Bao, L., Rose, L., Summers, J., and Ding, W. (2022). Malaria modeling and optimal control using sterile insect technique and insecticide-treated net. *Applicable Analysis*, 101(5):1715–1734.

Castillo-Chavez, C., Zhilan, F., and Wenzhang, H. (2002). On the computation of R_0 and its role on global stability. *Mathematical approaches for emerging and reemerging infectious diseases: an introduction*, 1(2):229–250.

Castro, M. C. (2017). Malaria transmission and prospects for malaria eradication: the role of the environment. *Cold Spring Harbor Perspectives in Medicine*, 7(10):a025601.

Chitnis, N., Hyman, J. M., and Cushing, J. M. (2008a). Determining important parameters in the spread of malaria through the sensitivity analysis of a mathematical model. *Bulletin of Mathematical Biology*, 70(5):1272–1296.

Chitnis, N., Smith, T., and Steketee, R. (2008b). A mathematical model for the dynamics of malaria in mosquitoes feeding on a heterogeneous host population. *Journal of Biological Dynamics*, 2(3):259–285.

Chiyaka, C., Garira, W., and Dube, S. (2009). Effects of treatment and drug resistance on the transmission dynamics of malaria in endemic areas. *Theoretical Population Biology*, 75(1):14–29.

Coffield, J., Daniel, J., Spagnuolo, A. M., Capouellez, R., and Stryker, G. A. (2023). A mathematical model for Chagas disease transmission with neighboring villages. *Frontiers in Applied Mathematics and Statistics*, 9(1):1225137.

Darteh, E. K. M., Buabeng, I., and Akuamoah-Boateng, C. (2021). Uptake of intermittent preventive treatment in pregnancy for malaria: further analysis of the 2016 Ghana Malaria Indicator Survey. *Journal of Public Health*, 29(158):967–978.

Dhangadamajhi, G., Kar, S. K., and Ranjit, M. (2010). The survival strategies of malaria parasite in the red blood cell and host cell polymorphisms. *Malaria Research and Treatment*, 2010(1):973094.

Dietz, K., Molineaux, L., and Thomas, A. (1974). A malaria model tested in the African savannah. *Bulletin of the World Health Organization*, 50(3-4):347.

Diouf, I., Fonseca, B. R., Caminade, C., Thiaw, W. M., Deme, A., Morse, A. P., Ndione, J.-A., Gaye, A. T., Diaw, A., and Ndiaye, M. K. N. (2020). Climate variability and malaria over West Africa. *The American Journal of Tropical Medicine and Hygiene*, 102(5):1037.

Djogbénou, L., Labbé, P., Chandre, F., Pasteur, N., and Weill, M. (2009). Ace-1 duplication in Anopheles gambiae: a challenge for malaria control. *Malaria Journal*, 18(8):61–70.

Donnelly, M. J., Corbel, V., Weetman, D., Wilding, C. S., Williamson, M. S., and Black, W. C. (2009). Does kdr genotype predict insecticide-resistance phenotype in mosquitoes? *Trends in Parasitology*, 25(5):213–219.

Edi, C. V., Djogbenou, L., Jenkins, A. M., Regna, K., Muskavitch, M. A., Poupardin, R., Jones, C. M., Essandoh, J., Ketoh, G. K., Paine, M. J., et al. (2014). CYP6 P450 enzymes and ACE-1 duplication produce extreme and multiple insecticide resistance in the malaria mosquito Anopheles gambiae. *PLoS Genetics*, 10(3):e1004236.

Elnour, Z., Grethe, H., Siddig, K., and Munga, S. (2023). Malaria control and elimination in Kenya: economy-wide benefits and regional disparities. *Malaria Journal*, 22(1):117.

Faulde, M. K., Rueda, L. M., and Khaireh, B. A. (2014). First record of the Asian malaria vector Anopheles stephensi and its possible role in the resurgence of malaria in Djibouti, Horn of Africa. *Acta Tropica*, 139(1):39–43.

Gething, P. W., Patil, A. P., Smith, D. L., Guerra, C. A., Elyazar, I. R., Johnston, G. L., Tatem, A. J., and Hay, S. I. (2011). A new world malaria map: Plasmodium falciparum endemicity in 2010. *Malaria Journal*, 10(378):1–16.

Griffin, J. T., Hollingsworth, T. D., Okell, L. C., Churcher, T. S., White, M., Hinsley, W., Bousema, T., Drakeley, C. J., Ferguson, N. M., Basáñez, M.-G., et al. (2010). Reducing Plasmodium falciparum malaria transmission in Africa: a model-based evaluation of intervention strategies. *PLoS Medicine*, 7(8):e1000324.

Group, W. B. (2021). Life expectancy at birth, total (years). Technical report. https://data.worldbank.org/indicator/SP.DYN.LE00.IN.

Hancock, P. A., Wiebe, A., Gleave, K. A., Bhatt, S., Cameron, E., Trett, A., Weetman, D., Smith, D. L., Hemingway, J., Coleman, M., et al. (2018). Associated patterns of insecticide resistance in field populations of malaria vectors across Africa. *Proceedings of the National Academy of Sciences*, 115(23):5938–5943.

Herdicho, F. F., Chukwu, W., Tasman, H., et al. (2021). An optimal control of malaria transmission model with mosquito seasonal factor. *Results in Physics*, 25(1):104238.

Huijben, S. and Paaijmans, K. P. (2018). Putting evolution in elimination: winning our ongoing battle with evolving malaria mosquitoes and parasites. *Evolutionary Applications*, 11(4):415–430.

Johnston, G. L., Smith, D. L., and Fidock, D. A. (2013). Malaria's missing number: calculating the human component of R_0 by a within-host mechanistic model of Plasmodium falciparum infection and transmission. *PLoS Computational Biology*, 9(4):e1003025.

Karger, D. N., Schmatz, D. R., Dettling, G., and Zimmermann, N. E. (2019). High resolution monthly precipitation and temperature timeseries for the period 2006-2100. *Scientific Data*, 7(1):248.

Keno, T. D., Dano, L. B., and Makinde, O. D. (2022). Modeling and optimal control analysis for malaria transmission with role of climate variability. *Computational and Mathematical Methods*, 2022(1):9667396.

Kenya, N. (2020). Kenya national malaria strategy 2019–2023. Nairobi, 2019. https://nmcp.or.ke/download/kenya-malaria-strategy-2019-2023/.

Khan, M. A., Shah, S. W., Ullah, S., and Gómez-Aguilar, J. F. (2019). A dynamical model of asymptomatic carrier zika virus with optimal control strategies. *Nonlinear Analysis: Real World Applications*, 50(1):144–170.

Koella, J. C. (1991). On the use of mathematical models of malaria transmission. *Acta Tropica*, 49(1):1–25.

Lacave, C. (2023). Malaria is thriving in Kenya thanks to climate change. https://www.gavi.org/vaccineswork/malaria-thriving-kenya-thanks-climate-change. [Accessed 03-09-2024].

Le Sueur, D. and Sharp, B. L. (1988). The breeding requirements of three members of the Anopheles gambiae Giles complex (Diptera: Culicidae) in the endemic malaria area of Natal, South Africa. *Bulletin of Entomological Research*, 78(4):549–560.

Li, J., Welch, R., Nair, U. S., Sever, T., Irwin, D., Cordon-Rosales, C., and Padilla, N. (2002). Dynamic malaria models with environmental changes. In *Proceedings of the Thirty-Fourth Southeastern Symposium on System Theory (Cat. No. 02EX540)*, pages 396–400. IEEE.

Long, C. A. and Zavala, F. (2017). Immune responses in malaria. *Cold Spring Harbor Perspectives in Medicine*, 7(8):a025577.

Macdonald, G. (1956). Epidemiological basis of malaria control. *Bulletin of the World Health Organization*, 15(3-5):613.

Maharaj, R. (2003). Life table characteristics of Anopheles arabiensis (Diptera: Culicidae) under simulated seasonal conditions. *Journal of Medical Entomology*, 40(6):737–742.

malERA Consultative Group on Vector Control (2011). A research agenda for malaria eradication: vector control. *PLoS Medicine*, 8(1):e1000401.

Mandal, S., Sarkar, R. R., and Sinha, S. (2011). Mathematical models of malaria-a review. *Malaria Journal*, 10(202):1–19.

Metchanun, N. (2020). *Evaluating Novel Vector Control Strategies: Modeling the impact of gene editing for malaria elimination in the Democratic Republic of Congo*. PhD thesis, Dissertation, Bonn, Rheinische Friedrich-Wilhelms-Universität, 2020.

Mieguim Ngninpogni, D., Ndo, C., Ntonga Akono, P., Nguemo, A., Nguepi, A., Metitsi, D. R., Tombi, J., Awono-Ambene, P., and Bilong Bilong, C. F. (2021). Insights into factors sustaining persistence of high malaria transmission in forested areas of sub-Saharan Africa: the case of Mvoua, south Cameroon. *Parasites & Vectors*, 14(2):1–10.

Mitchell, S. N., Stevenson, B. J., Müller, P., Wilding, C. S., Egyir-Yawson, A., Field, S. G., Hemingway, J., Paine, M. J., Ranson, H., and Donnelly, M. J. (2012). Identification and validation of a gene causing cross-resistance between insecticide classes in Anopheles gambiae from Ghana. *Proceedings of the National Academy of Sciences*, 109(16):6147–6152.

Mohammed-Awel, J., Agusto, F., Mickens, R. E., and Gumel, A. B. (2018). Mathematical assessment of the role of vector insecticide resistance and feeding/resting behavior on malaria transmission dynamics: Optimal control analysis. *Infectious Disease Modelling*, 3(1):301–321.

Mohammed-Awel, J. and Gumel, A. B. (2023). Can insecticide resistance increase malaria transmission? a genetics-epidemiology mathematical modeling approach. *Journal of Mathematical Biology*, 87(2):28.

Montoya, C. and Romero-Leiton, J. P. (2020). Mathematical modelling for malaria under resistance and population movement. *Revista Integración*, 38(2):133–163.

Mordecai, E. A., Caldwell, J. M., Grossman, M. K., Lippi, C. A., Johnson, L. R., Neira, M., Rohr, J. R., Ryan, S. J., Savage, V., Shocket, M. S., et al. (2019). Thermal biology of mosquito-borne disease. *Ecology Letters*, 22(10):1690–1708.

Ngandu, C. B., Momberg, D., Magan, A., Chola, L., Norris, S. A., and Said-Mohamed, R. (2020). The association between household socio-economic status, maternal socio-demographic characteristics and adverse birth and infant growth outcomes in sub-Saharan Africa: a systematic review. *Journal of Developmental Origins of Health and Disease*, 11(4):317–334.

Ngarakana-Gwasira, E. T., Bhunu, C. P., Masocha, M., and Mashonjowa, E. (2016). Assessing the role of climate change in malaria transmission in Africa. *Malaria Research and Treatment*, 2016(1):7104291.

Ngonghala, C. N. (2022). Assessing the impact of insecticide-treated nets in the face of insecticide resistance on malaria control. *Journal of Theoretical Biology*, 555:111281.

Ngonghala, C. N., Ngwa, G. A., and Teboh-Ewungkem, M. I. (2012). Periodic oscillations and backward bifurcation in a model for the dynamics of malaria transmission. *Mathematical Biosciences*, 240(1):45–62.

Nkiruka, O., Prasad, R., and Clement, O. (2021). Prediction of malaria incidence using climate variability and machine learning. *Informatics in Medicine Unlocked*, 22:100508.

Nyawanda, B. O., Beloconi, A., Khagayi, S., Bigogo, G., Obor, D., Otieno, N. A., Lange, S., Franke, J., Sauerborn, R., Utzinger, J., et al. (2023). The relative effect of climate variability on malaria incidence after scale-up of interventions in western Kenya: A time-series analysis of monthly incidence data from 2008 to 2019. *Parasite Epidemiology and Control*, 21:e00297.

Olutimo, A., Mbah, N., Abass, F., and Adeyanju, A. (2024). Effect of environmental immunity on mathematical modeling of malaria transmission between vector and host population. *Journal of Applied Sciences and Environmental Management*, 28(1):205–212.

Orwa, T. O., Mbogo, R. W., and Luboobi, L. S. (2021). Optimal control analysis of hepatocytic-erythrocytic dynamics of *plasmodium falciparum* malaria. *Infectious Disease Modelling*, 7(1):82–108.

Paaijmans, K. P., Cator, L. J., and Thomas, M. B. (2013). Temperature-dependent pre-bloodmeal period and temperature-driven asynchrony between parasite development and mosquito biting rate reduce malaria transmission intensity. *PLoS ONE*, 8(1):e55777.

Parham, P. E. and Michael, E. (2010). Modelling climate change and malaria transmission. *Modelling Parasite Transmission and Control*, 673(1):184–199.

Patz, J., Githeko, A., McCarty, J., Hussein, S., Confalonieri, U., De Wet, N., et al. (2003). Climate change and infectious diseases. *Climate Change and Human Health: Risks and Responses*, 2(1):103–132.

Pongtavornpinyo, W., Yeung, S., Hastings, I. M., Dondorp, A. M., Day, N. P., and White, N. J. (2008). Spread of anti-malarial drug resistance: mathematical model with implications for act drug policies. *Malaria Journal*, 7(229):1–12.

Pontryagin, L. S. (2018). *Mathematical theory of optimal processes*. Routledge.

R Core Team (2024). *R: A Language and Environment for Statistical Computing*. R Foundation for Statistical Computing, Vienna, Austria.

Riveron Miranda, J., Tchouakui, M., Mugenzi, L., Menze, B., Chiang, M.-C., and Wondji, C. (2018). *Insecticide resistance in malaria vectors: an update at a global scale*. IntechOpen.

Romero-Leiton, J. P. and Ibargüen-Mondragón, E. (2019). Stability analysis and optimal control intervention strategies of a malaria mathematical model. *Applied Sciences*, 21(1):184–218.

Ross, R. (1911). *The prevention of malaria*. John Murray, London.

Saddler, A. and Koella, J. C. (2015). Modelling the impact of declining insecticide resistance with mosquito age on malaria transmission. *Malariaworld Journal*, 6(1):13.

Sheldon, B. C. and Verhulst, S. (1996). Ecological immunology: costly parasite defences and trade-offs in evolutionary ecology. *Trends in Ecology & Evolution*, 11(8):317–321.

Stein, M. (1987). Large sample properties of simulations using Latin Hypercube Sampling. *Technometrics*, 29(2):143–151.

Su, X.-z., Zhang, C., and Joy, D. A. (2020). Host-malaria parasite interactions and impacts on mutual evolution. *Frontiers in Cellular and Infection Microbiology*, 10:587933.

Sultana, M., Sheikh, N., Mahumud, R. A., Jahir, T., Islam, Z., and Sarker, A. R. (2017). Prevalence and associated determinants of malaria parasites among Kenyan children. *Tropical Medicine and Health*, 45(1):1–9.

Sutherst, R. W. (2004). Global change and human vulnerability to vector-borne diseases. *Clinical Microbiology Reviews*, 17(1):136–173.

Tchoumi, S., Kouakep, Y., Mbogne, D., Kamgang, J., and Tchuenche, J. (2021). Optimal control of a malaria model with long-lasting insecticide-treated nets. *Mathematical Modelling and Control*, 1(4):188–207.

Tchoumi, S. Y., Chukwu, C., Diagne, M. L., Rwezaura, H., Juga, M., and Tchuenche, J. M. (2022). Optimal control of a two-group malaria transmission model with vaccination. *Network Modeling Analysis in Health Informatics and Bioinformatics*, 12(7):1–19.

Tchoumi, S. Y., Kamgang, J. C., Tieudjo, D., and Sallet, G. (2018). A basic general model of vector-borne diseases. *Communications in Mathematical Biology and Neuroscience*, 2018(3).

Torres-Sorando, L. and Rodrıguez, D. J. (1997). Models of spatio-temporal dynamics in malaria. *Ecological Modelling*, 104(2-3):231–240.

Tumwiine, J., Mugisha, J., and Luboobi, L. (2007). On oscillatory pattern of malaria dynamics in a population with temporary immunity. *Computational and Mathematical Methods in Medicine*, 8(3):191–203.

Tuno, N., Farjana, T., Uchida, Y., Iyori, M., and Yoshida, S. (2023). Effects of temperature and nutrition during the larval period on life history traits in an invasive malaria vector Anopheles stephensi. *Insects*, 14(6):543.

USAID (2017). President's malaria initiative: Kenya malaria operational plan fy 2018. U.S. global malaria coordinator and the national malaria control programs and partners. Technical report. https://reliefweb.int/report/kenya/president-s-malaria-initiative-kenya-malaria-operational-plan-fy-2018.

Wang, Y., Gilbreath III, T. M., Kukutla, P., Yan, G., and Xu, J. (2011). Dynamic gut microbiome across life history of the malaria mosquito Anopheles gambiae in Kenya. *PLoS ONE*, 6(9):e24767.

WHO (2015). World malaria report 2014: summary. Technical report, World Health Organization. https://www.who.int/publications/i/item/9789241564830.

WHO (2018). High burden to high impact: a targeted malaria response. Technical report, World Health Organization. https://www.who.int/publications/i/item/WHO-CDS-GMP-2018.25.

WHO (2021). WHO global technical strategy for malaria 2016–2030. Technical report, World Health Organization. https://www.who.int/publications/i/item/9789240031357.

WHO (2023). WHO malaria policy advisory group (mpag) meeting report, 18–20 april 2023. Technical report, World Health Organization. https://www.who.int/publications/i/item/9789240074385#:~:text=Overview,by%20the%20Global%20Malaria%20Programme.

WHO (2024). World malaria report 2024. Technical report, World Health Organization. https://www.who.int/teams/global-malaria-programme/reports/world-malaria-report-2024.

WHO guidelines, W. (2023). WHO guidelines for malaria, 14 march 2023. Technical report, World Health Organization. https://iris.who.int/handle/10665/366432.

Wu, J., Dhingra, R., Gambhir, M., and Remais, J. V. (2013). Sensitivity analysis of infectious disease models: methods, advances and their application. *Journal of the Royal Society Interface*, 10(86):20121018.

Yanda, P. Z., Wandiga, S. O., Kangalawe, R. Y., Opondo, M., Olago, D., Githeko, A., Downs, T., Kabumbuli, R., Opere, A., Githui, F., et al. (2006). Adaptation to climate change/variabilityinduced highland malaria and cholera in the Lake Victoria region. In *Assessments of Impacts and Adaptations to Climate Change (AIACC)*.

Yang, H. M. and Ferreira, M. U. (2000). Assessing the effects of global warming and local social and economic conditions on the malaria transmission. *Revista de Saude Publica*, 34(3):214–222.

Appendices

Appendix A: Similarity Report

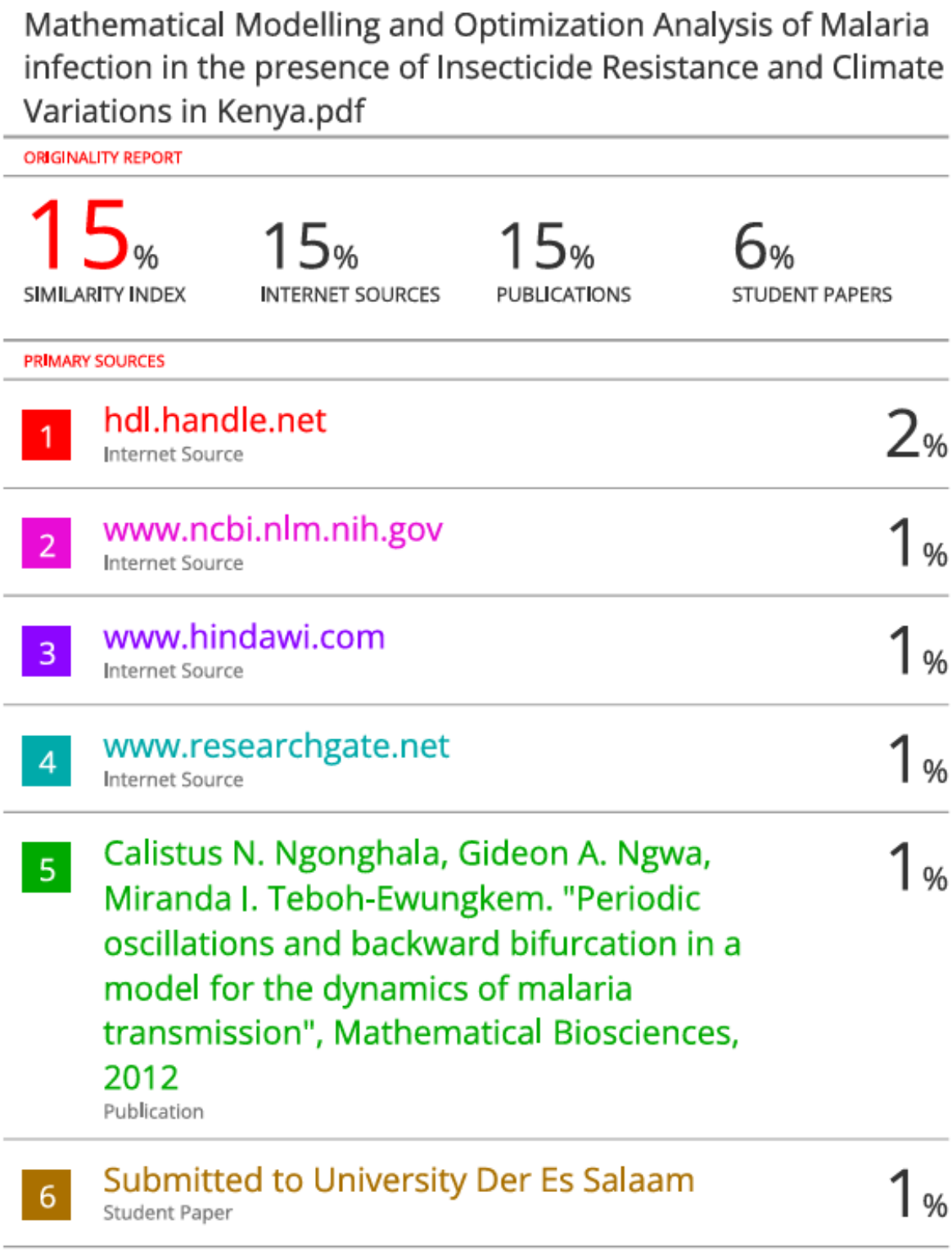

Mathematical Modelling and Optimization Analysis of Malaria infection in the presence of Insecticide Resistance and Climate Variations in Kenya.pdf

ORIGINALITY REPORT

15%	15%	15%	6%
SIMILARITY INDEX	INTERNET SOURCES	PUBLICATIONS	STUDENT PAPERS

PRIMARY SOURCES

1	hdl.handle.net Internet Source	2%
2	www.ncbi.nlm.nih.gov Internet Source	1%
3	www.hindawi.com Internet Source	1%
4	www.researchgate.net Internet Source	1%
5	Calistus N. Ngonghala, Gideon A. Ngwa, Miranda I. Teboh-Ewungkem. "Periodic oscillations and backward bifurcation in a model for the dynamics of malaria transmission", Mathematical Biosciences, 2012 Publication	1%
6	Submitted to University Der Es Salaam Student Paper	1%

7	ir.knust.edu.gh Internet Source	1 %
8	rguir.inflibnet.ac.in:8080 Internet Source	1 %
9	www.mdpi.com Internet Source	1 %
10	Jemal Mohammed-Awel, Abba B. Gumel. "Can insecticide resistance increase malaria transmission? A genetics-epidemiology mathematical modeling approach", Journal of Mathematical Biology, 2023 Publication	1 %
11	Submitted to Strathmore University Student Paper	<1 %
12	Ngonghala, Calist. "Mathematical Modeling and Analysis of Epidemiological and Chemical Systems", Proquest, 2012. Publication	<1 %
13	Submitted to Higher Education Commission Pakistan Student Paper	<1 %
14	coek.info Internet Source	<1 %
15	Kumama Regassa Cheneke. "Optimal Control and Bifurcation Analysis of HIV Model",	<1 %

Appendix B: Ethical Clearance Confirmation

Strathmore UNIVERSITY

14th November 2024

Ms Chepkemoi Lorna,
lorna.chepkemoi@strathmore.edu

Dear Ms Chepkemoi,

RE: Mathematical Modeling and Optimization Analysis Considering Insecticide Resistance and Climate Variations in Kenya

This is to inform you that SU-ISERC has reviewed and **approved** your above **SU-masters** proposal. Your application reference number is **SU-ISERC2433/24.** The approval period is from **14th November 2024 to 13th November 2025.**

This approval is subject to compliance with the following requirements:

i. Only approved documents including (informed consents, study instruments, MTA) will be used.
ii. All changes including (amendments, deviations, and violations) are submitted for review and approval by SU-ISERC.
iii. Death and life-threatening problems and serious adverse events or unexpected adverse events whether related or unrelated to the study must be reported to SU-ISERC within 72 hours of notification.
iv. Any changes anticipated or otherwise that may increase the risks or affected safety or welfare of study participants and others or affect the integrity of the research must be reported to SU-ISERC within 72 hours.
v. Clearance for the export of biological specimens must be obtained from relevant institutions.
vi. Submission of a request for renewal of approval at least 60 days prior to the expiry of the approval period. Attach a comprehensive progress report to support the renewal.
vii. Submission of an executive summary report within 90 days of completion of the study to SU-ISERC.

Before commencing your study, you will be expected to obtain a research license from National Commission for Science, Technology, and Innovation (NACOSTI) https://research-portal.nacosti.go.ke/ and obtain other clearances needed.

Yours sincerely,

Mr Ambrose Rachier,
Chairperson; SU-ISERC

Ole Sangale Rd, Madaraka Estate. PO Box 59857-00200, Nairobi, Kenya. Tel +254 (0)703 034000
Email admissions@strathmore.edu www.strathmore.edu

Appendix C: Numerical methods

Fourth Order Runge-Kutta Method

The formula for the fourth order Runge-Kutta method is given by

$$y_{n+1} = y_n + \frac{h}{6}(k_1 + 2k_2 + 2k_3 + k_4) \tag{10}$$

where the slope estimates k_1,k_2,k_3,k_4 are calculated as follows:

$$k_1 = hf(x_n, y_n) \tag{11}$$

$$k_2 = hf\left(x_n + \frac{h}{2}, y_n + \frac{k_1}{2}\right) \tag{12}$$

$$k_3 = hf\left(x_n + \frac{h}{2}, y_n + \frac{k_2}{2}\right) \tag{13}$$

$$k_4 = hf(x_n + h, y_n + k_3) \tag{14}$$

k_1,k_2,k_3 and k_4 correspond to slope estimates at the beginning, middle and end of the interval, respectively.

Butcher's Fifth Order Runge-Kutta Method

The formula for the fifth order Runge-Kutta method is given by

$$y_{n+1} = y_n + \frac{h}{90}(7k_1 + 32k_3 + 12k_4 + 32k_5 + 7k_6) \tag{15}$$

where the slope estimates k_1,k_2,k_3,k_4, k_5, k_6 are calculated as follows:

$$k_1 = f(x_n, y_n) \tag{16}$$

$$k_2 = f\left(x_n + \frac{h}{4}, y_n + \frac{h}{4}k_1\right) \tag{17}$$

$$k_3 = f\left(x_n + \frac{h}{4}, y_n + \frac{h}{8}k_1 + \frac{h}{8}k_2\right) \tag{18}$$

$$k_4 = f\left(x_n + \frac{h}{2}, y_n - \frac{h}{2}k_2 + k_3 h\right) \tag{19}$$

$$k_5 = f\left(x_n + \frac{3}{4}h, y_n + \frac{3}{16}k_1h + \frac{9}{16}k_4h\right) \tag{20}$$

$$k_6 = f\left(x_n + h, y_n + \frac{3}{7}k_1h + \frac{2}{7}k_2h + \frac{12}{7}k_3h - \frac{12}{7}k_4h + \frac{8}{7}k_5h\right) \tag{21}$$

Forward-Backward Sweep Method

The Forward–backward sweep method (FBSM) is an iterative numerical technique for solving the two-point boundary value problem (TPBVP) that arises from Pontryagin's Maximum Principle.

Forward-backward sweep method algorithm

Let $x = x_1, ..., x_{n+1}$ and $\lambda = \lambda_1, ..., \lambda_{n+1}$ be the vector approximations for the state and adjoint. **Step 1.** Create an initial guess for the control u over the interval.

Step 2. Using the initial condition $x(t_0) = x_0$ and the values for u, solve x forward in time.

Step 3. Using the transversality condition $\lambda(t_1) = 0$ and the values for u and x, solve λ backward in time as given to its equation in the optimality system.

Step 4. Update u by entering the new x and λ values into the characterization of the optimal control.

Appendix D: Numerical Simulation of Optimal Control Problem

Personal protection $u_1 \neq 0$, treatment $u_2 = 0$, and vaccination $u_3 = 0$

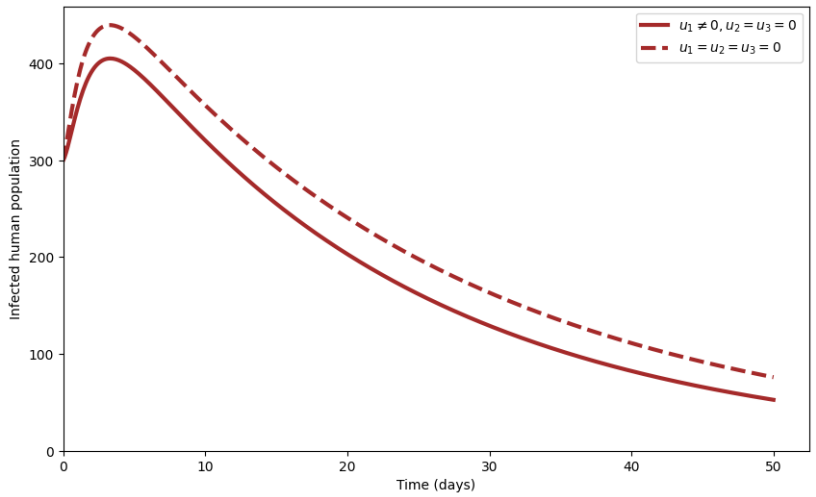

(a) Infected humans

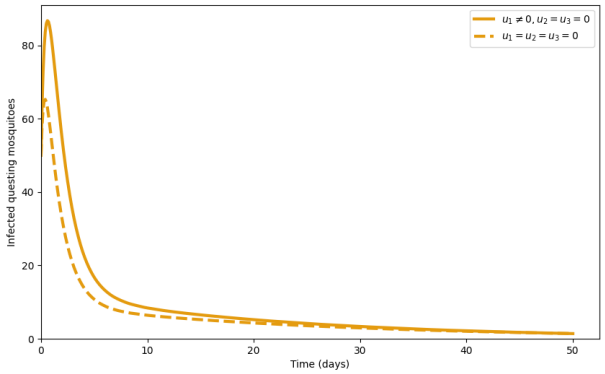

(b) Infected questing mosquitoes

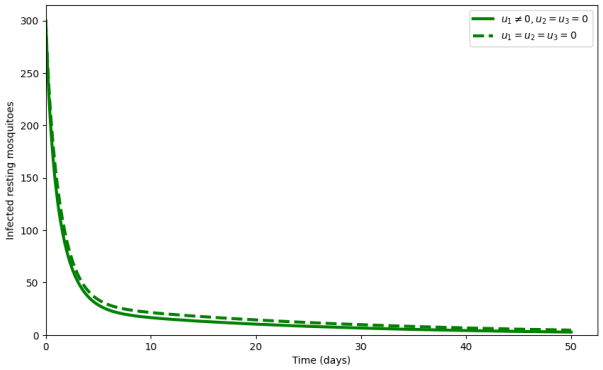

(c) Infected questing mosquitoes

Figure A.1: Graph showing the effect of implementing personal protection u_1 only as a control measure on infected human and mosquito population.

Personal Protection $u_1 = 0$, Treatment $u_2 \neq 0$, and Vaccination $u_3 = 0$

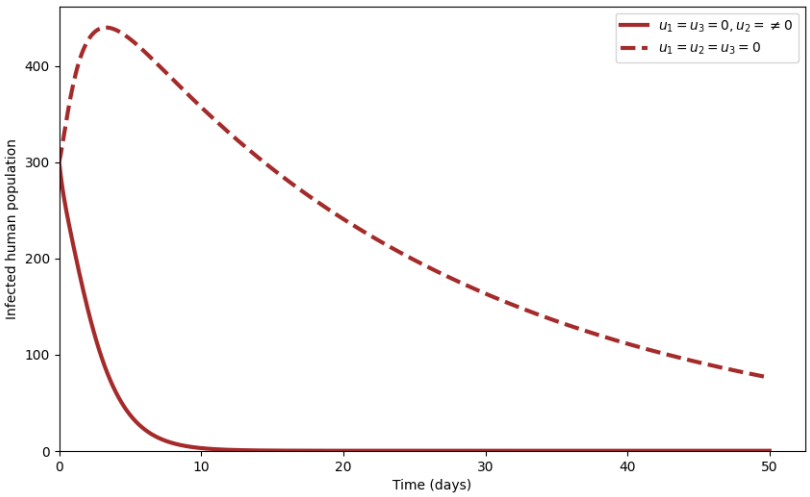

(a) Infected humans

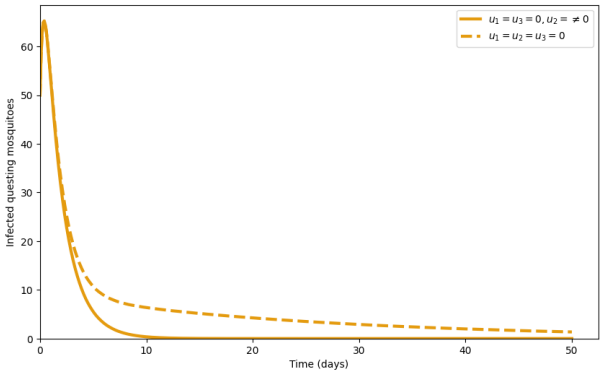

(b) Infected questing mosquitoes

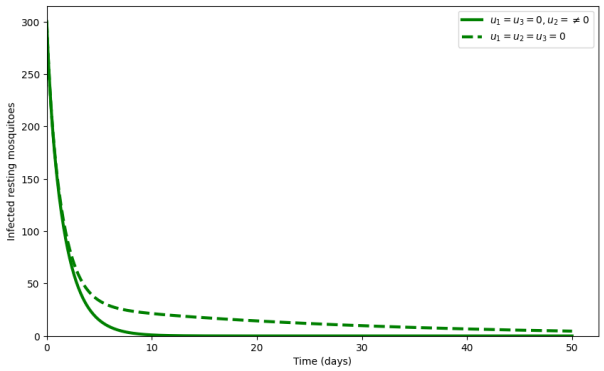

(c) Infected questing mosquitoes

Figure A.2: Graph showing the effect of implementing treatment u_2 only as a control measure on infected human and mosquito population.

Personal Protection $u_1 = 0$, Treatment $u_2 = 0$, and Vaccination $u_3 \neq 0$

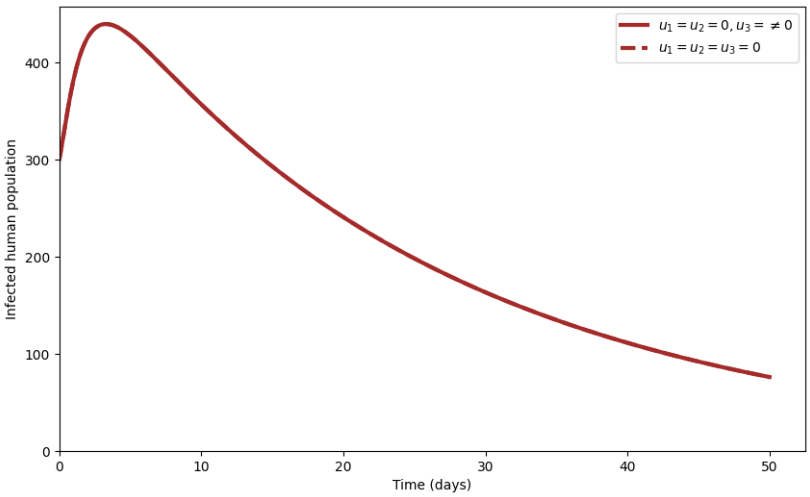

(a) Infected humans

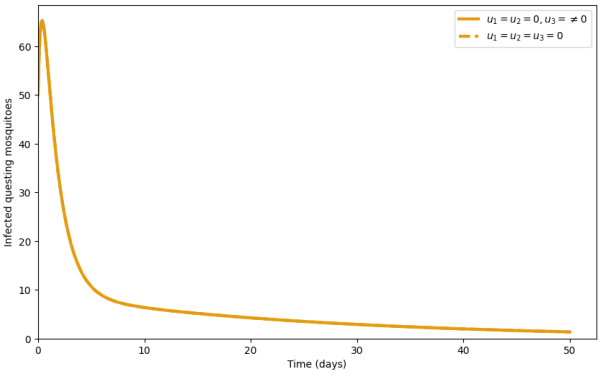

(b) Infected questing mosquitoes

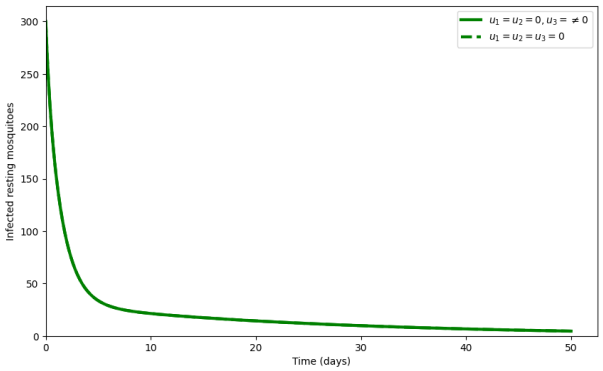

(c) Infected questing mosquitoes

Figure A.3: Graph showing the effect of implementing vaccination u_3 only as a control measure on infected human and mosquito population.

Appendix E: Samples of used Simulation Codes

```
Numerical simulation without climate dependent variables
"""

# imports
import numpy as np
import matplotlib.pyplot as plt
from scipy.integrate import odeint
import pandas as pd

# Parameters
N_h = 10000 # Humans
N_v = 1000 # Mosquitoes
beta_h = 0.5#2.5  #transmission from mosquitoes to humans
beta_v = 2.5  # transmission from humans to mosquitoes
b = 5 #Mosquito biting rate
gamma_h = 0.05 #recovery rate
mu_h = 0.00004559    # Natural death rate of humans
delta_h = 0.0002  #death rate due to infection in humans
mu_v = 0.05      #natural death rate of mosquitoes
delta_v = 0#0.4862#0.2562#0.4862 #mosquito death rate due to
   insecticide
#0.0476
alpha_h = 0.4559   # Human birth rate
alpha_v = 0.6

# Transition rates for resting/questing mosquitoes
alpha_s = 0.6666  #resting rate for susceptible mosquitoes
omega = 0.8 #return rate to questing mosquitoes
alpha_i = 0.6666 #resting rate for infected mosquitoes
p = 0.6    #transition rate to resting
q = 0.5  #transition rate for infected mosquitoes
p_1 = 0.5
q_1 = 0.6
```

```
33
34 # Initial conditions
35 S_h0=7000; I_h0=300 ; S_r0=800; S_q0=300; I_r0= 200; I_q0=50
36 initial_conditions=[S_h0,I_h0,S_r0,S_q0,I_r0,I_q0]
37
38 # Time_span
39 # Time range
40 t_span = (0, 100)
41 t_eval = np.linspace(0, 100, 1000)
42
43
44 def si_mosquito_model_with_resting(time, y, N_h, N_v, beta_v,
       beta_h, gamma_h, mu_h, delta_h,
45                                    mu_v, alpha_s, alpha_i,
                                          alpha_h, omega, delta_v,
                                          alpha_v,
46                                    b, p, q, p_1, q_1):
47     S_h, I_h, S_r, S_q, I_r, I_q = y
48     # Human equations
49     dSHdt = alpha_h + gamma_h * I_h - b * beta_h * S_h * (I_q /
           N_h) - mu_h * S_h
50     dIHdt = b * beta_h * S_h * (I_q / N_h) - mu_h * I_h - delta_h
           * I_h - gamma_h * I_h
51
52     # Mosquito equations (susceptible and infected)
53     dSQdt = omega * S_r - mu_v * S_q - alpha_s * b * (S_h / N_h)
           * S_q - alpha_i * b * S_q * (I_h / N_h) - delta_v * S_q
54     dIQdt = omega * I_r - mu_v * I_q - alpha_s * b * I_q * (S_h /
           N_h) - alpha_i * b * I_q * (I_h / N_h) - delta_v * I_q
55     dSRdt = alpha_v * N_v + p * alpha_s * b * (S_h / N_h) * S_q -
           omega * S_r - mu_v * S_r - delta_v * S_r
56     dIRdt = q * alpha_i * b * S_q * (I_h / N_h) + p_1 * b * (S_h
           / N_h) * alpha_s * I_q + q_1 * b * alpha_i * I_h / N_h *
           I_q - mu_v * I_r - omega * I_r - delta_v * I_r
```

```
57
58      return [dSHdt, dIHdt, dSRdt, dSQdt, dIRdt, dIQdt]
59
60  from scipy.integrate import solve_ivp
61
62  solution = solve_ivp(
63      fun=lambda t, y: si_mosquito_model_with_resting(
64          t, y, N_h, N_v, beta_v, beta_h, gamma_h, mu_h, delta_h,
65          mu_v, alpha_s, alpha_i, alpha_h, omega, delta_v, alpha_v,
66          b, p, q, p_1, q_1),
67      t_span=t_span,
68      y0=initial_conditions,
69      method='RK45',
70      t_eval=t_eval
71  )
72
73  # Convert solution to DataFrame
74  df = pd.DataFrame(solution.y.T, columns=[
75      'Susceptible humans', 'Infected humans',
76      'Susceptible resting', 'Susceptible questing',
77      'Infected resting', 'Infected questing'
78  ])
79  df['Time'] = solution.t
80
81  # Preview
82  df.head(10)
83
84  #Use of insecticides
85  df.to_csv('dataframe1.csv', index=False)
86
87  #No use of insecticides (delta_v=0)
88  df.to_csv('dataframe2.csv', index=False)
89
90  """Use of insecticides
```

```
91
92  Human population
93  """
94
95  import matplotlib.pyplot as plt
96
97  # Extract time and solution
98  time = solution.t  # time points (from t_eval)
99  y = solution.y     # solution array; each row corresponds to one
        variable
100
101 # Extract S_h (first row in solution matrix)
102 S_h = y[0]  # Susceptible humans
103
104 # Plot
105 plt.plot(time, S_h, color='blue', label='Susceptible Humans')
106 plt.xlim(left=0)
107 plt.xlabel('Time (days)')
108 plt.ylabel('Susceptible human population')
109 plt.show()
110
111 # Extract time and solution
112 time = solution.t  # time points (from t_eval)
113 y = solution.y     # solution array; each row corresponds to one
        variable
114
115 I_h = y[1]  # Infected humans
116
117 # Plot
118 plt.plot(time, I_h, color='red')
119 plt.xlim(left=0)
120 plt.ylim(bottom=0)
121 plt.xlabel('Time (days)')
122 plt.ylabel('Infected human population')
```

```
plt.show()

"""Mosquito population when insecticide is used"""

# Extract time and solution
time = solution.t
y = solution.y

S_r = y[2]  # Susceptible resting

# Plot
plt.plot(time, S_r, color='blue')
plt.xlim(left=0)
plt.xlabel('Time (days)')
plt.ylabel('Susceptible resting mosquitoes')
plt.show()

# Extract time and solution
time = solution.t
y = solution.y

I_r = y[4]  # infected resting

# Plot
plt.plot(time, I_r, color='red')
plt.xlim(left=0)
#plt.ylim(bottom=0)
plt.xlabel('Time (days)')
plt.ylabel('Infected resting mosquitoes')
plt.show()
```